Hindawi
Journal of Food Biochemistry
Volume 2023, Article ID 5671679, 19 pages
https://doi.org/10.1155/2023/5671679

*Research Article*

# Expectorant Effects of Immature Asian Pear Extract on $PM_{2.5}$-Induced Subacute Pulmonary Injury in Mice

**Bertoka Fajar Surya Perwira Negara**,[1] **Joo Wan Kim**,[2] **Khawaja Muhammad Imran Bashir**,[3] **Jin-Hwa Lee**,[4] **Mo-Un Ku**,[5] **Ki-Young Kim**,[6] **Su Shin**,[6] **Eun-Jin Hong**,[6] **Sae-Kwang Ku**,[7] **and Jae-Suk Choi**[4]

[1]*Department of Food Biotechnology, College of Medical and Life Sciences, Silla University, 140, Baegyang-daero 700 beon-gil, Sasang-gu, Busan 46958, Republic of Korea*
[2]*Department of Companion Animal Health, Daegu Haany University, Gyeongsan-si, Gyeongsangbuk-do 38610, Republic of Korea*
[3]*German Engineering Research Center for Life Science Technologies in Medicine and Environment, Busan 46742, Republic of Korea*
[4]*Department of Seafood Science and Technology, The Institute of Marine Industry, Gyeongsang National University, 2-9, Tongyeonghaean-ro, Tongyeong-si, Gyeongsangnam-do 53064, Republic of Korea*
[5]*Department of Biomedical Laboratory Science, College of Health and Welfare, Kyungwoon University, Gumi 39160, Republic of Korea*
[6]*Research Institute, Bio Port Korea Inc., 36, Ballyongsandan 1-ro, Jangan-eup, Gijang-gun, Busan 46034, Republic of Korea*
[7]*Department of Anatomy and Histology, College of Korean Medicine, Daegu Haany University, Gyeongsan-si, Gyeongsangbuk-do 38610, Republic of Korea*

Correspondence should be addressed to Sae-Kwang Ku; gucci200@dhu.ac.kr and Jae-Suk Choi; jsc1008@gnu.ac.kr

Received 13 March 2023; Revised 2 June 2023; Accepted 8 June 2023; Published 22 June 2023

Academic Editor: Jae Young Je



This study investigated the expectorant effects of immature Asian pear extract (IAP; *Pyrus pyrifolia* Nakai) on subacute pulmonary injuries in Balb/c mice induced by particulate matter with a diameter of approximately 2.5 $\mu$m ($PM_{2.5}$). IAP was administered at three doses, namely, 400, 200, and 100 mg/kg. The body weight and weight gain changes, lung weights, lung and body surface gross inspections, tracheal secretions, and substance P and ACh content in lung tissue homogenate were observed one day after the tenth IAP administration. The mRNA expression of the genes related to mucus production and lung histopathology was compared with that of the negative and positive controls. Favorable pulmonary protective effects on $PM_{2.5}$-induced subacute pulmonary injuries, mucus overproduction, and respiratory acidosis were observed in groups treated with IAP at all three doses, possibly through potent anti-inflammatory and mucolytic expectorant activities mediated by the increase in the content of lung substances P and ACh and the downregulation of lung MUC5AC and MUC5B mRNA expression in a dose-dependent manner. The results of this study show that an appropriate oral administration of IAP has sufficient pulmonary protective effects and can be used as a candidate for the development of functional food ingredients.

## 1. Introduction

The rapid increase in particulate matter (PM), an air pollutant, has led to the emergence of various respiratory diseases in Korea, China, and Japan, as well as in other East Asian countries. Beijing, the capital of China, has a particularly high incidence of respiratory diseases caused by PM [1–3]. A large amount of PM, in the form of yellow dust, is generated in Northwest China in the spring, on the Loess Plateau, and in the deserts of Inner Mongolia, which

combines with automobile exhaust and coal gas to form a more severe form of PM as it passes through the inland industrial areas of China [4]. Since the 2008 Beijing Olympics, Beijing has drawn attention as one of the area most seriously affected by PM worldwide, and measures to reduce air pollution have been undertaken [5]. When measured on the ground, the majority of PM consisted of PM with a diameter of approximately 2.5 $\mu$m ($PM_{2.5}$) and contained mineral dust including organic and inorganic contaminants [6].

Inhalation of PM causes serious lung damage and secondary heart damage and triggers allergic inflammation, the most frequent and serious cause of asthma [7]. Asthma is the most representative noncollective inflammatory airway disease caused by air pollution [1–3, 8]. According to WHO [9], the prevalence of asthma reached nearly 235 million cases worldwide in 2017. In addition, the accumulation of PM increases oxidative stress in the epithelial cells of the airway and lung tissues, leading to local tissue damage and inflammatory responses [5, 10]. More than 70% of inhaled PM accumulates in the lower trachea, and approximately 22% reaches the alveoli [10]. Accumulated PM affects epithelial cells in the airway and lung tissue, causing local tissue damage and inflammatory responses because of oxidative stress [5, 10]. The initiation of an inflammatory response is marked by an increase in inflammatory mediators and proinflammatory cytokines [11]. Reactive oxygen species (ROS), catalase (CAT), heme oxygenase-1 (HO-1), superoxide dismutase (SOD), and glutathione peroxidase (GPX) [12] are factors influencing oxidative stress.

Coughing (sneezing) is defined as a spurt reflex following the obstruction of the epiglottis that is related to sound characteristics [13]. Cough can cause various respiratory disorders, and chronic cough is known to reduce the patients' quality of life, necessitating prompt and proper treatment [14]. Bronchoconstriction is one of the main causes of coughing. It provokes rapidly adapting receptors (RARs) intrapulmonary, which regulate cough induction by increasing cough sensitivity [15]. The activation of the early adaptation receptors in the lung induces bronchoconstriction and the secretion of mucus through the parasympathetic reflexes [16]. Cough is subdivided into nonmucus-secreting (dry) or mucus-secreting (thoracic and wet recurrent) cough [16]. Antitussives are effective against dry cough; however, they are not effective against wet recurrent cough unless accompanied by expectorant action [17]. The inflammatory response also participates in the induction of several respiratory diseases, including cough [18, 19]. Drugs exhibiting concurrent expectorant, anti-inflammatory, and antitussive effects can be used effectively in various respiratory disorders, especially bronchial asthma, cough, and respiratory inflammatory diseases caused by toxic environmental substances [20–25]. Expectorants have been used in the treatment of various respiratory systems as they promote mucous secretion in the body, relieve clumped sputum, and act as an airway lubricant [26, 27]. Its effect has been evaluated based on mucus secretion using various methods. The most commonly used method is the pH-sensitive phenol red tracheal secretion measurement method [20].

The metabolite of bromhexine ambroxol[2-amino-3,5-dibromo-N-(trans-4-hydroxycyclohexyl)benzylamine] is a representative expectorant that dissolves sputum by promoting respiratory secretion [28, 29]. It has been prescribed clinically for several respiratory diseases for more than 40 years. Ambroxol has a secretotropic mucolytic action in addition to the antioxidant, anti-inflammatory, antiviral, and antibacterial activities of ambroxol hydrochloride (AM) [29, 30]. However, the use of this drug in patients with gastric ulcers and pregnant women is strictly controlled [31]. In this study, according to the results of drug efficacy evaluation in various previous lung injury models [22–25, 29], the AM (250 mg/kg) oral administered group was selected as the control drug group.

Respiratory disorders caused by PM are a growing concern; thus, the development of drugs for prevention or treatment of the respiratory damage due to PM has been undertaken [2, 3]. Physiologically active substances derived from natural products have excellent anti-inflammatory and antioxidant activities and relatively fewer side effects [32]. Therefore, there has been increased interest in the development of respiration protective drugs using natural products in $PM_{2.5}$-induced lung injury models [1–3, 12]. Among these, pears (*Pyrus* spp.) are well-known as commonly consumed fruits worldwide [33]. Pears can be consumed in the form of beverages, purees, jellies, or jams; however, they are mostly consumed as fresh fruit [34]. Unlike other fruits, such as apples, grapes, and tangerines, pears do not have a unique color and scent; therefore, studies on the chemical substances or biological activities in pears are relatively rare [35]. Based on updated research on the chemical substances present in *P. pyrifolia* Nakai, the most common oriental pear cultivated in Korea, caffeoyl triterpenes [36], a phenylpropanoid malate derivative [37], and other phenolic compounds, such as flavonoids, have been found as major active compounds [37–40]. The content of chlorogenic acid, caffeic acid, arbutin, phenolic compounds, malaxinic acid, flavonoids, and antioxidants, which are major compounds in pears, decreases with maturation [41]. Thus, the antioxidant activity and amount of phenolic compounds in immature pears are significantly higher than in mature pears [35]. Immature fruits are removed immediately after flowering through fruit thinning to harvest high-quality mature fruits [38], a process in which only one of the seven or eight clusters of fruit is left intact; the remaining are discarded [42]. Considering the mature pear production in Korea [43], the number of unprocessed immature pears is estimated to be approximately 15,000 tons per year [35], with most of these pears being completely discarded [35]. Therefore, it is beneficial to separate active components of immature embryos for the development of functional food materials [35].

This study investigated the expectorant activity of immature Asian pear extract (IAP) using a $PM_{2.5}$-induced mouse lung injury model [1–3], a representative PM-induced respiratory disorder experimental animal model, to develop functional food materials or natural drugs that can effectively improve respiratory functions. The representative sputum samples were compared with those of the

oral administration group, which received 250 mg/kg of AM, a soluble expectorant [22–25, 29], as a control.

## 2. Materials and Methods

*2.1. Test Material.* The IAP (immature Asian pear; *Pyrus pyrifolia* Nakai) extract was supplied from Bioport Korea Inc. (Yangsan-si, Korea). The light brown powder of IAP extract can be mixed in distilled water to make a solution (40 mg/mL). The solutions were stored at −20°C until further use. A part of the IAP extract powder (IAP2022BPK01) was listed as a sample in the herbarium of the Medical Research Center for Herbal Convergence on Liver Disease, Daegu Haany University (Gyeongsan, Korea). AM was purchased from Sigma-Aldrich (St. Louis, MO, USA) and used as the control drug [29].

*2.2. Administration of the Test Substance.* Prior to the administration, the IAP solutions were prepared by dissolving the extract with distilled water and making various concentrations (40, 20, and 10 mg/mL). Subsequently, the solutions were administered orally once daily using a metal sonde attached to a 1 mL syringe at a dose of 10 mL/kg (400, 200, and 100 mg/kg) for 10 days. In the same way, distilled water was used for preparing the AM solution (25 mg/mL), and a dose of 10 mL/kg (250 mg/kg) was administered orally once daily for 10 days. To ensure the same handling for $PM_{2.5}$ control and normal vehicles, the sterile distilled water was only administered orally along with the vehicle in the control group. The AM concentration of 250 mg/kg was chosen according to previous studies [22–25, 29].

*2.3. High-Performance Liquid Chromatography Analyses.* The amount of arbutin in the IAP extract was analyzed using the 1200 series Agilent HPLC (Agilent Technologies, Inc., Santa Clara, CA, USA), G1314B detector (Agilent Technologies, Inc.), and C18 column (4.6 mm × 250 mm, 5 $\mu$m; Capcell Pak column; Osaka Soda Co. Ltd., Osaka, Japan). Standard arbutin (Alfa Aesar; Massachusetts, USA) and IAP extract were diluted in the mobile phase solvent consisting of 10 mM $KH_2PO_4$ and acetonitrile in a ratio of 98.9 : 1.1. A 0.45-$\mu$m membrane filter was used to filtrate the mobile phase before use. During analysis, the arbutin was analyzed at 280 nm, and the column was maintained at 30°C. A 10 $\mu$L sample was injected at a flow rate of 0.8 mL/min, and the results were quantitatively analyzed.

*2.4. Experimental Animals.* Seventy-two SPF/VAF inbred Balb/c male mice (Orient Bio, Seungnam, Korea) were acclimated for 10 days. Ten mice were grouped into each of the six groups based on their body weight (average weight: normal vehicle control group, 21.38 ± 1.06 g; $PM_{2.5}$-induced lung damage experimental group, 21.39 ± 0.97 g) one day before the first intranasal injection of $PM_{2.5}$ and the start of test substance administration. The experiment was conducted after receiving approval from the Daegu Haany University Animal Experiment Ethics Committee (Approval No. DHU2022-097). All experimental animals fasted for 18 h before starting the administration of the test substance and on the final day of necropsy. Water was provided ad libitum during that time. For an inflammatory mouse model (inflammation, asthma, bronchiectasis, etc.), an IAP dose of 200 mg/kg was administered. Doses of 400 and 100 mg/kg were selected as high and low doses, respectively, at a common ratio of 2.

*2.5. Experimental Groups.* Six groups were included in the current study. Mice were sacrificed at the end of each experiment.

Group 1 (intact control): oral administration of 10 mL/kg of distilled water with intranasal instillation of 0.1 ml/kg of saline

Group 2 ($PM_{2.5}$ control): oral administration of 10 mL/kg of distilled water with intranasal instillation of 1 mg/kg of $PM_{2.5}$

Group 3 (AM250): oral administration of 250 mg/kg of AM with intranasal instillation of 1 mg/kg of $PM_{2.5}$

Group 4 (IAP400): oral administration of 400 mg/kg of IAP with intranasal instillation of 1 mg/kg of $PM_{2.5}$

Group 5 (IAP200): oral administration of 200 mg/kg of IAP with intranasal instillation of 1 mg/kg of $PM_{2.5}$

Group 6 (IAP100): oral administration of 100 mg/kg of IAP with intranasal instillation of 1 mg/kg of $PM_{2.5}$

*2.6. Induction of Lung Damage.* $PM_{2.5}$ was diluted in physiological saline to 10 mg/mL, following the previous studies [1–3, 25]. Subacute lung injury was induced via the intranasal instillation of this suspension at a dose of 0.1 mL/kg (1 mg/kg) twice at a 48 h interval (Day 0 and Day 2). The intranasal instillation was performed 1 h before the oral administration of the test substance. In group 1, the same amount of vehicle (physiological saline) was instilled intranasally instead of the $PM_{2.5}$ suspension to ensure the same handling, restraint, and administration stress. Sonication was performed using an ultrasonicator (Branson, St. Louis, MO, USA) for 30 min before intranasal injection to prevent excessive aggregation of $PM_{2.5}$ in the suspension.

*2.7. Measurement of Tracheal Secretion.* Tracheal secretion was measured as described in the previous studies [20, 22–25]. Twenty-four hours after the tenth administration of IAP or AM, 10 mL/kg of 5% pH-sensitive phenol red (Junsei Chemical Co. Ltd., Tokyo, Japan) solution (w/v) dissolved in physiological saline was administered intraperitoneally. After 30 min, a rodent inhalation anesthesia apparatus (Surgivet, Waukesha, WI, USA) and a rodent ventilator (Harvard Apparatus, Cambridge, UK) under 3% isoflurane, 70% $N_2O$, and 28.5% $O_2$ mixed gas inhalation anesthesia were used to visually observe the degree of redness on the body surface. The body surface was photographed using a FinePix S700 camera (Fujifilm, Tokyo, Japan). The trachea (from thyroid cartilage to the tracheal

bifurcation) was excised, immersed in 1 mL of physiological saline, and sonicated using 5210 Branson Ultrasonics (St. Louis, MO, USA) for 15 min to prepare a tracheal lavage solution. Subsequently, 1 mL of $NaHCO_3$ solution (5%, w/v; Sigma-Aldrich, St. Louis, MO, USA) was added, and the optical density was read using a Sunrise microplate reader (Tecan, Männedorf, Switzerland) at 546 nm.

*2.8. Extraction of Lung Tissue.* The entire lungs of each test animal were removed, the tracheas were resected, and an automatic scale (Precisa Instrument, Dietikon, Switzerland) was used to measure the weight 24.5 h following the tenth dose of the test substance and 30 min after a single intraperitoneal administration of phenol red. For RT-PCR and P and ACh content analyses, three right lung lobes (upper, middle, and lower) were used, while for histopathological observation and gross lesions, the left lobe of the lung was used.

## 3. Observation Items

*3.1. Body Weight.* The body weight measurement was done every day before $PM_{2.5}$ administration until sacrifice using an electronic balance. To minimize the deviation in weight, all the animals fasted overnight on the day before and the last day of administration.

*3.2. Body Surface Observation and Measurement of Tracheal Secretion and Lung Weight.* A single intraperitoneal injection of a pH-sensitive dye and phenol red (5%; Junsei Chemical Co. Ltd., Tokyo, Japan) solution dissolved in saline (*w*/*v*) at a concentration of 10 mL/kg was administered 24 h after the last administration of the test substance and 30 min after the injection of phenol red solution to measure the tracheal secretion. Gross image acquisition was performed using the FinePix S700 camera (Fujifilm, Tokyo, Japan) to observe the body surface redness under anesthesia with 2-3% isoflurane (Hana Pharm. Co., Hwasung, Korea) in a mixture of 70% $N_2O$ and 28.5% $O_2$. A rodent inhalation anesthesia apparatus (Surgivet, Waukesha, WI, USA) and rodent ventilator (Harvard Apparatus, Cambridge, UK) were used to induce and maintain anesthesia. Subsequently, the intensity of the redness on individual body surfaces on the acquired gross digital images was measured using the *i*Solution FL ver 9.1 image analyzer (IMT *i*-solution Inc., Burnaby, BC, Canada) and calculated as a percentage (%) of the intact control.

The trachea, from the thyroid cartilage to the main-stem bronchi, was removed. Following ultrasonication for 15 min using an ultrasonicator (Model 5210, Branson Ultrasonics, Danbury, CT, USA), 1 mL of $NaHCO_3$ solution (5%, *w*/*v*) was added to normal saline, and the optical density of the prepared TLF was measured at 546 nm using a microplate reader (Model Sunrise, Tecan, Männedorf, Switzerland) as described previously [20] with some modifications. The lungs were separated under inhalational anesthesia after tracheal dissection, and the weights of the individual lungs were analyzed using the XB320M balance (Precisa Instrument, Dietikon, Switzerland). The body weight to relative weight was also calculated.

*3.3. Lung Gross Necropsy Findings (the Ratio of the Congested to Healed Area, %).* Ligations with 3-0 nylon (3-0 sterilized nylon thread, NB 324, AILEE, Pusan, Korea) were performed on the left secondary bronchus after weighing the separated lung. The upper, middle, and lower lobes of the right lung were used for substance P and ACh content and RT-PCR analyses. The left lobes were used for gross and histopathological inspections in the current experiment. Gross inspections were performed using a commercial digital camera (FinePix S700; Fujifilm, Tokyo, Japan). Subsequently, the congestional regions (%) in the individual left-lung lobes on the gross digital images were measured using a computer-based automated image analyzer (*i*Solution FL ver 9.1, IMT *i*-solution Inc., Burnaby, BC, Canada).

*3.4. Substance P and Ach Content Assay in the Lung.* The lung tissues of the upper, middle, and lower lobes of the right lungs were homogenized using a bead beater (Taco™Pre, GeneResearch Biotechnology Corp., Taichung, Taiwan) and an ultrasonic cell disruptor (Madell Technology Corp., Ontario, CA, USA) in an equal volume of normal saline and stored at −150°C using an ultradeep freezer (Sanyo, Tokyo, Japan) until analysis. The lung tissue homogenates were centrifuged at 12,500 rpm for 30 min at 4°C using a cryocentrifuge (Gyrozen, Daejeon, Korea), and the supernatant substance P and ACh contents were measured using mouse substance P (Mybiosource, San Diego, CA, USA) and ACh (Mybiosource, San Diego, CA, USA) ELISA kits according to the manufacturer's protocol. The optical density was measured at 450 nm using a microplate reader.

*3.5. mRNA Expression in the Lung Tissue (Real-Time RT-PCR).* mRNA expression of the genes involved in mucus production, MUC5AC (Muc5ac) and MUC5B (Muc5b), was measured using RT-PCR as described in previous studies [25, 44, 45]. RNA was extracted using the TRIzol reagent (Invitrogen, Carlsbad, CA, USA). The samples were treated with recombinant DNase I (DNA-free; DNA-free DNA Removal kit; Thermo Fisher Scientific Inc., Rockford, IL, USA) to prevent contamination with DNA, and RNA was reverse-transcribed using the High-Capacity cDNA Reverse Transcription Kit (Thermo Fisher Scientific Inc., Rockford, IL, USA) according to the manufacturer's instructions. The PCR primers include CCACTTTCTCCTTCTCCACACC and GGTTGTCGATGCAGCCTTGCTT (GenBank Accession no. NM_010844), CTGAAGACCTGTCGGAACCCAA and GCCACACACTTCATCTGGTCCT (GenBank Accession no. NM_028801), and CATTGCTGACAGGATGCA GAAGG and TGCTGGAAGGTGGACAGTGAGG (GenBank Accession no. NM_007393) for MUC5AC, MUC5B, and $\beta$-actin gene, respectively. The analysis was performed using the Real-Time System (Bio-Rad, Hercules, CA, USA). The following thermal conditions were applied according to the manufacturer's suggestion: 50°C for 2 min (activation),

95°C for 10 min (pre-soak), 95°C for 15 sec (denaturation), 60°C for 1 min (annealing), 95°C for 15 sec, 60°C for 15 sec, and 95°C for 15 sec (melting curve). The data were normalized to $\beta$-actin (Actb) mRNA expression using the comparative threshold cycle method [46]. All qPCR primer pairs were obtained from OriGene Technologies (Rockville, MD).

*3.6. Histopathological and Histoimmunological Changes in the Lungs.* The left lobe of the lung was fixed in 10% neutral buffered formalin for 24 h and embedded in paraffin blocks. Tissue slides were prepared from the fixed tissue using an automatic tissue cutter (RM2255; Leica Biosystems, Nussloch, Germany). After H&E staining of tissue slides, the mean ASA (%/mm$^2$) reflected the pulmonary functions' gas exchange capacities [22–25, 47, 48]. The mean alveolar septal thickness ($\mu$m), the number of inflammatory cells in the alveolar regions (cells/mm$^2$), and the number of PAS-positive mucus-producing cells in the secondary bronchus [22–25, 47–49] were calculated for general histomorphometrical analysis using a computer-assisted image analysis program and camera system. The histological fields observed in this inspection were selected as the upper regions of the secondary bronchus, with 10 histological lung fields in each group.

A separate tissue slide was subjected to avidin-biotin-peroxidase complex (ABC)-based immunohistochemical staining to measure the caspase-3 and COX-2 levels using the vectastain elite ABC kit (Vector Lab., Burlingame, CA, USA) and examined with a computer-assisted automated image analyzer. The endogenous peroxidase activity was analyzed using a peroxidase substrate kit (Vector Lab., Burlingame, CA, USA) according to the manufacturer' instruction. After heating-based epitope retrieval (95–100°C) in 10 mM citrate buffer (pH 6.0), the nonspecific binding of immunoglobulin was blocked by incubation in the normal horse serum blocking solution for 1 h in a humidity chamber [25, 50, 51].

Anti-cleaved caspase-3 antibody (Cell Signaling Technology Inc., Beverly, MA, USA) and anti-COX-2 (murine) polyclonal antibody (Cayman Chemical., Ann Arbor, MI, USA) were used in this study. Primary antisera were incubated overnight at 4°C in a humidity chamber and then incubated with biotinylated universal secondary antibodies and ABC reagents for 1 h at room temperature in a humidity chamber. Lastly, the sections were reacted with the peroxidase substrate kit for 3 min at room temperature. All sections were rinsed in 0.01 M phosphate-buffered saline (PBS) three times between each step. In this study, cells with more than 20% immunoreactivity and a high density of cleaved caspase-3 and COX-2 were considered positive. The number of cleaved caspase-3 and COX-2-immunolabeled cells located in the restricted view field of the lung parenchyma, around the alveolar septum, and secondary bronchus mucosa regions (cells/mm$^2$) was measured using a computer-based automated image analyzer and histological camera system, as described in previous reports [25, 50, 51]. The histopathologist was blinded to the group distribution during the analysis.

*3.7. Statistics.* All values are expressed as the mean ± standard deviation ($n = 10$). The significance between the groups was verified ($p < 0.05$) with one-way analysis of variance (ANOVA) using the SPSS program (Release 18.0, SPSS Inc., Chicago, IL, USA). Variance homogeneity was assessed using the Leven test. The significance ($p < 0.05$) was verified using Tukey's honest significant difference (THSD) test if no significant difference was observed. The significance ($p < 0.05$) was verified using Dunnett's T3 (DT3) test [52] if a significant deviation was observed.

## 4. Results

*4.1. Arbutin Content in the IAP Extract.* The HPLC analysis of the IAP extract used in this study showed that arbutin was detected at a concentration of 8.60 mg/g in the IAP extract (Figure 1).

*4.2. Changes in Body Weight.* Compared with that in group 1, no significant changes in body weight or weight gain were observed in any of the $PM_{2.5}$-induced lung injury experimental groups. No significant changes in body weight and weight gain were observed in groups 3, 4, 5, or 6 compared with those in group 2 (Table 1 and Figure 2).

*4.3. Changes in Tracheal pH-Sensitive Phenol Red Secretion.* A significant ($p < 0.01$) increase in the OD value and phenol red secretion of TLF was observed in group 2 compared with those in group 1. A significant ($p < 0.01$) increase in the tracheal phenol red secretion was observed in a dose-dependent manner in groups 4, 5, and 6. In particular, group 5 showed a greater increase in the OD value of TLF and phenol red secretion compared with those in group 3 (Figure 3).

*4.4. Changes Observed on the Body Surface via the Naked Eye Observation.* A significant ($p < 0.01$) decrease in the body surface redness, which indicates respiratory acidosis (decrease in pH) caused by an increase in the carbon dioxide saturation due to dyspnea [25, 53–55], was observed in group 2 compared with that in group 1. However, compared with that in group 2, a significant ($p < 0.01$) increase in the body surface redness was observed in a dose-dependent manner in groups 4, 5, and 6. In particular, group 5 exhibited activity in the reduction of $PM_{2.5}$-induced body surface redness comparable with that of group 3 (Figure 4 and Figure 5).

*4.5. Lung Macroscopic Necropsy Findings and Changes in Weight.* Lung enlargement with significant local congestion and a significant ($p < 0.01$) increase in the gross congestion area and absolute and relative lung weights were observed in group 2 compared with those in group 1. However, marked reductions in gross congestion in the lungs and absolute and relative weights were observed in a dose-dependent manner in groups 4, 5, and 6 compared with those of group 2. In

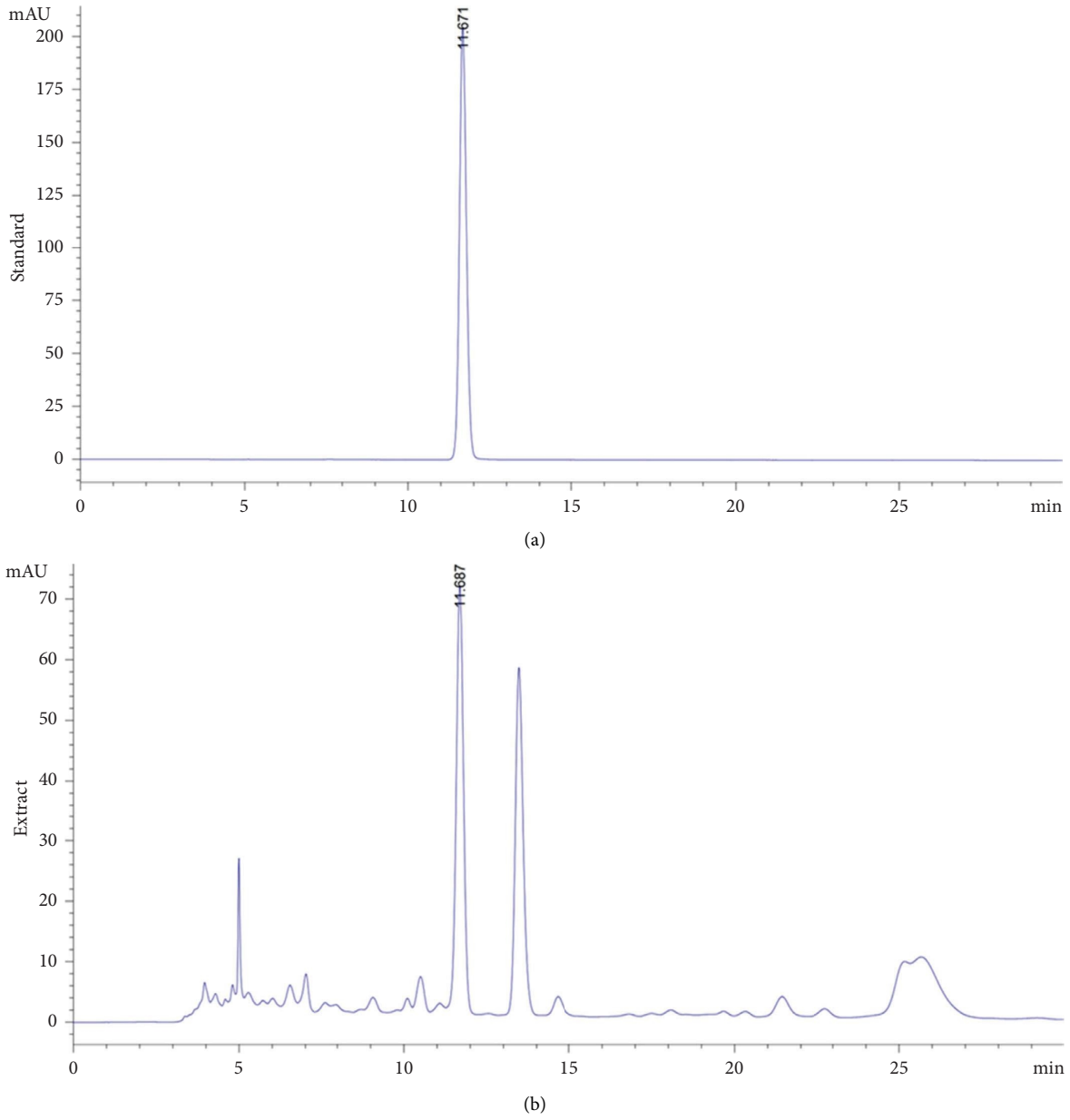


Figure 1: Profile arbutin: (a) standard and (b) immature Asian pear extract.

particular, group 5 exhibited activity similar to that of group 3 in suppressing $PM_{2.5}$-induced pulmonary congestion, enlargement, and an increase in absolute and relative weight (Table 2 and Figure 6).

*4.6. Changes in Substance P and ACh Content in Lung Tissue.* A significant ($p < 0.01$) increase in substance P and Ach content in the lung tissue was observed in group 2 compared with that in group 1. A significant ($p < 0.01$ or $p < 0.05$) increase in substance P and ACh content in lung tissue was observed in a dose-dependent manner in groups 4, 5, and 6 compared with that in group 2. In particular, group 5 showed an increase in substance P and ACh content in lung tissue comparable with that of group 3 (Figure 7).

*4.7. Changes in MUC5AC and MUC5B mRNA Expression Related to Mucus Production in Lung Tissue.* A significant ($p < 0.01$) increase in the expression of MUC5AC and MUC5B mRNA related to mucus production in the lung tissue was observed in group 2 compared with that in group 1. However, a significant ($p < 0.01$) decrease in MUC5AC and MUC5B mRNA expression in the lung tissue was observed in a dose-dependent manner in groups 4, 5, and 6 compared with that in group 2. In particular, group 5 inhibited the increase in MUC5AC and MUC5B mRNA expression related to mucus production to a similar extent as group 3 (Figure 8).

*4.8. Histopathological Changes in the Lungs.* Marked fleshy lesions (thickening of the alveolar septum due to infiltration of inflammatory cells, thickening of the secondary bronchial

Table 1: Body weight gains in intact or $PM_{2.5}$-treated pulmonary injured mice.

| Groups | Body weights (g) at periods | | | |
|---|---|---|---|---|
| | Initial test article administration [A]* | Last $10^{th}$ test article administration | 24 h after last $10^{th}$ test article administration [B]* | Body weight gains [B-A] |
| Controls | | | | |
| Intact vehicle | 18.85 ± 0.84 | 22.55 ± 1.02 | 20.34 ± 0.78 | 1.49 ± 0.43 |
| $PM_{2.5}$ | 19.24 ± 0.72 | 22.72 ± 0.75 | 20.76 ± 0.92 | 1.52 ± 0.63 |
| Reference-AM | | | | |
| 250 mg/kg | 18.93 ± 0.82 | 22.79 ± 0.73 | 20.54 ± 0.71 | 1.61 ± 0.63 |
| Test substance-IAP | | | | |
| 400 mg/kg | 18.89 ± 1.23 | 22.92 ± 1.70 | 20.46 ± 1.47 | 1.57 ± 0.47 |
| 200 mg/kg | 18.94 ± 0.67 | 22.71 ± 0.69 | 20.49 ± 0.60 | 1.55 ± 0.55 |
| 100 mg/kg | 18.90 ± 0.91 | 22.39 ± 0.95 | 20.43 ± 1.25 | 1.53 ± 0.61 |

Values are expressed mean ± SD of 10 mice; $PM_{2.5}$ = diesel particulate matter NIST 1650b; AM = ambroxol hydrochloride; IAP = immature Asian pear (fruit of *Pyrus pyrifolia* Nakai cv. Shingo) extract; *all animals were overnight fasted (about 18 h; water was not restricted).

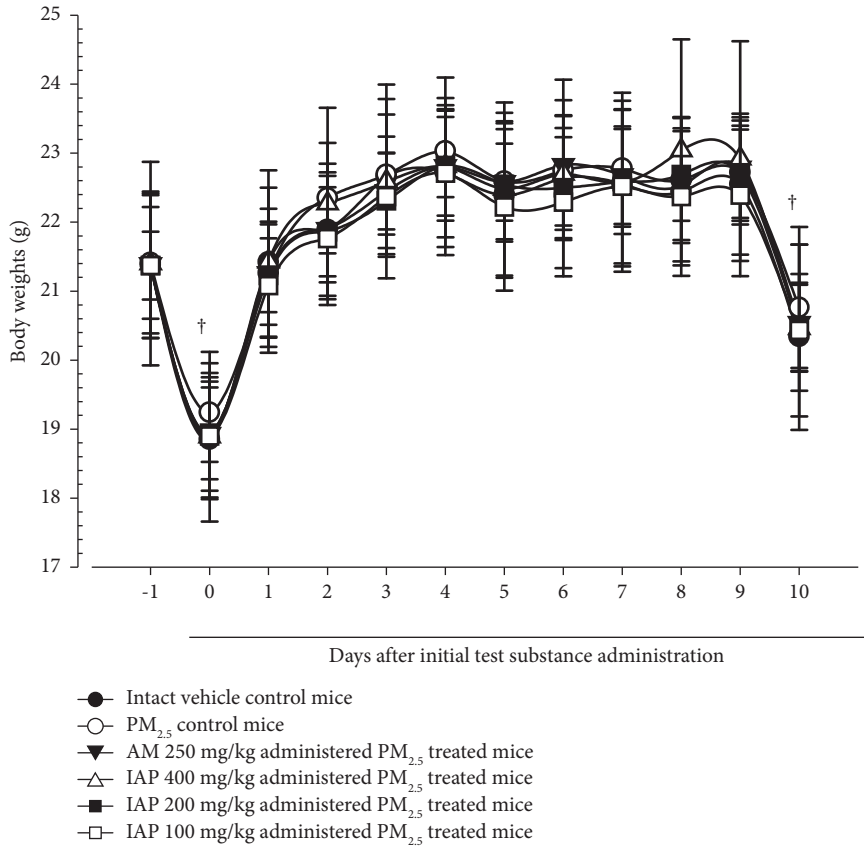


Figure 2: Body weights changes in Intact or $PM_{2.5}$-treated pulmonary injured mice. Values are expressed mean ± SD of 10 mice; $PM_{2.5}$ = diesel particulate matter NIST 1650b; AM = ambroxol hydrochloride; IAP = immature Asian pear (fruit of *Pyrus pyrifolia* Nakai cv. Shingo) extract. Test substances-IAP and reference-AM were orally administered, once a day for 10 days, respectively. Subacute pulmonary injuries were induced by intranasal instillation of $PM_{2.5}$ suspensions, twice 48 h-interval at day 0 and day 2, at a dose level of 1 mg/kg, respectively; day -1 means 1 day before initial test article administration; day 10 means the day of sacrifice, 24 h after last $10^{th}$ test article administration; all animals were overnight fasted before initial test article administration and sacrifice (†).

mucosa, and increased PAS-positive mucus-producing cells) were observed in group 2. A significant ($p < 0.01$) increase in the average alveolar septal and secondary bronchial mucosal thickness, the number of infiltrating inflammatory cells around the alveoli, the number of PAS-positive mucus-producing cells in the secondary bronchial mucosa, and the associated decrease in ASA were observed in group 2 compared with those in group 1. However, a significant ($p < 0.01$) increase in ASA, mean alveolar septum thickness, and a decrease in the number of infiltrating inflammatory cells around the alveoli were observed in groups 4, 5, and 6 compared with that in group 2. In particular, group 5

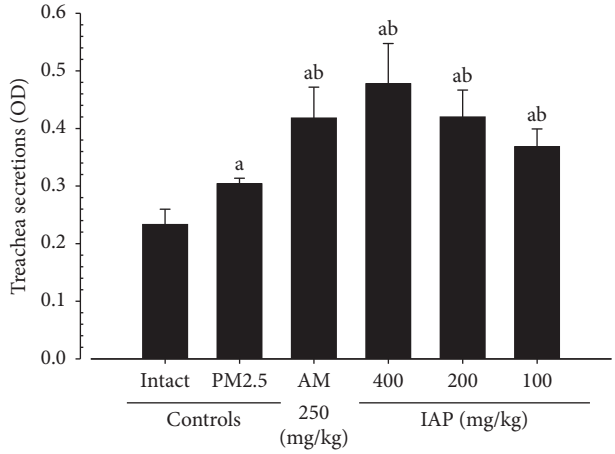


FIGURE 3: Trachea pH-sensitive phenol red secretions in intact or $PM_{2.5}$-treated pulmonary injured mice. Values are expressed mean ± SD of 10 mice; $PM_{2.5}$ = diesel particulate matter NIST 1650b; AM = ambroxol hydrochloride; IAP = immature Asian pear (fruit of *Pyrus pyrifolia* Nakai cv. Shingo) extract; TLF = trachea lavage fluid; OD = optical density; DT3 = Dunnett's T3; $^{a}p < 0.01$ as compared with intact vehicle control by DT3 test; $^{b}p < 0.01$ as compared with $PM_{2.5}$ control by DT3 test.

exhibited suppression of $PM_{2.5}$-induced alveolar septum thickening and inflammatory cell infiltration and reduction of ASA to an extent comparable with that of group 3. In addition, as part of the expectorant activity [220, 2–25], a significant ($p < 0.01$) increase in the mean thickness of the secondary bronchial mucosa and a number of PAS-positive mucus-producing cells was also observed in groups 4, 5, and 6 compared with those in group 2 in a dose-dependent manner. In particular, group 5 showed an increase in secondary bronchial mucosal thickness and the number of PAS-positive mucus-producing cells comparable with that of group 3 (Table 3 and Figure 9).

*4.9. Immunohistochemical Changes in the Lungs.* A significant ($p < 0.01$) increase in the number of cleaved caspase-3 associated with apoptosis and COX-2 immune response cells associated with inflammation was observed in the alveolar septum and secondary bronchial mucosa in group 2 compared with that in group 1. However, there was a significant ($p < 0.01$, $p < 0.05$) decrease in the number of cleaved caspase-3 and COX-2 immunoreactive cells around the alveolar septum and secondary bronchial mucosa in groups 4, 5, and 6 compared with that in group 2 in a dose-dependent manner. In particular, group 5 exhibited consistent inhibition of $PM_{2.5}$-induced apoptosis-related cleaved caspase-3 and inflammation-related COX-2 immune response cells in the alveolar septum and secondary bronchial mucosa comparable with that of group 3 (Table 4 and Figure 10).

## 5. Discussion

Due to the possibility of PM-induced damage to various organs, including the respiratory and cardiovascular systems [56, 57] and associated increases in mortality [58, 59], great attention has been focused on the harmful effects of PM. Among them, $PM_{2.5}$ is the greatest source of concern for public health [60]. The incidence of arteriosclerosis, respiratory diseases, and lung cancer increases significantly with exposure to high concentrations of $PM_{2.5}$ present in the air [8, 61–63]. Compared with $PM_{10}$, which is a form of dust approximately 10 $\mu$m in diameter, $PM_{2.5}$ can evade innate immunity due to its relatively smaller size; therefore, $PM_{2.5}$ can reach the deep respiratory tract, bronchi, and alveoli with greater ease, thereby, resulting in severe toxicity. Various toxic substances present in $PM_{2.5}$, such as endotoxins, polycyclic aromatic hydrocarbons, sulfates, and heavy metals, can also cause serious problems [64]. With the increase in the incidence of respiratory disorders caused by PM, there is a growing need to develop a treatment method for the treatment or prevention of PM-induced respiratory damage. In line with these needs, a $PM_{2.5}$-induced lung injury Balb/c mouse model has been established, which exhibits conditions similar to those in PM-induced respiratory diseases in humans [2, 3, 25, 64]. The development of respiratory protection drugs using natural products in $PM_{2.5}$-induced lung injury models has gained popularity [1–3], as bioactive substances derived from natural products have relatively fewer side effects and excellent anti-inflammatory and antioxidant activities [32].

Pears (*Pyrus* spp.) are one of the most commonly consumed fruits worldwide [33]. The content of major active ingredients, such as arbutin, chlorogenic acid, malaxinic acid, total caffeic acid, total flavonoids, total phenolic compounds, and antioxidant activity decreases with maturation [41]. Thus, the content of phenolic compounds in immature pears and their related antioxidant activity are significantly higher than those in mature pears [35]. Therefore, the potential for separating physiologically active components from immature embryos and developing functional food materials is very high [35].

Therefore, in this study, the dose-dependent expectorant activity of IAP was evaluated using a $PM_{2.5}$-induced mouse lung injury model [1–3, 25], a representative PM-induced respiratory disorder experimental animal model, for developing functional food materials or natural drugs that are

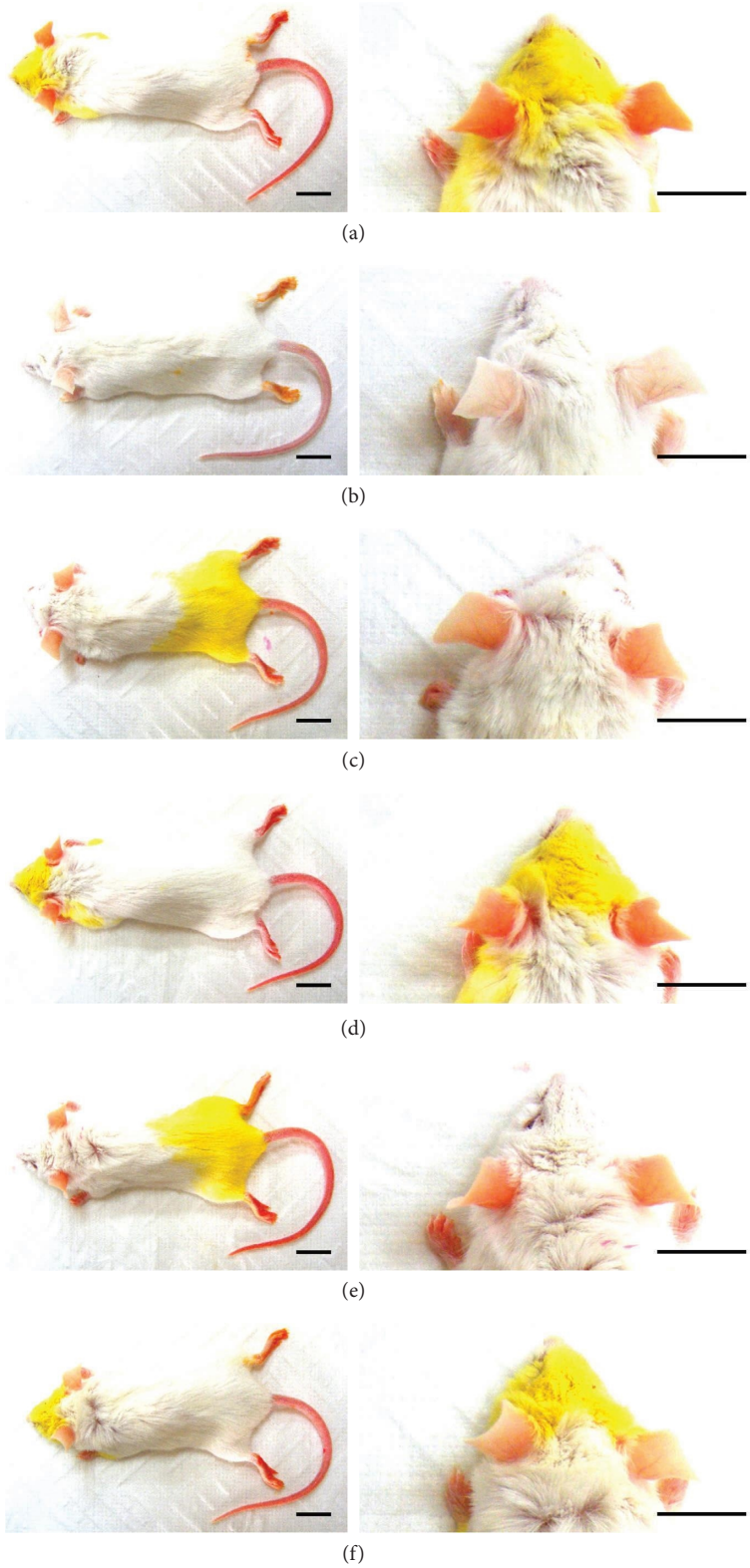


FIGURE 4: Representative skin surface gross images, taken from Intact or $PM_{2.5}$-treated pulmonary injured mice. (a) Intact vehicle control (distilled water orally administered mice with saline intranasal instillation); (b) $PM_{2.5}$ control (distilled water orally administered mice with $PM_{2.5}$ intranasal instillation); (c) AM250 (250 mg/kg of AM orally administered mice with $PM_{2.5}$ intranasal instillation); (d) IAP200 (200 mg/kg of IAP orally administered mice with $PM_{2.5}$ intranasal instillation); (e) IAP100 (100 mg/kg of IAP orally administered mice with $PM_{2.5}$ intranasal instillation); (f) IAP50 (50 mg/kg of IAP orally administered mice with $PM_{2.5}$ intranasal instillation); $PM_{2.5}$ = diesel particulate matter NIST 1650b; AM = ambroxol hydrochloride; IAP = immature Asian pear (fruit of *Pyrus pyrifolia* Nakai cv. Shingo) extract; scale bars = 12.00 mm.

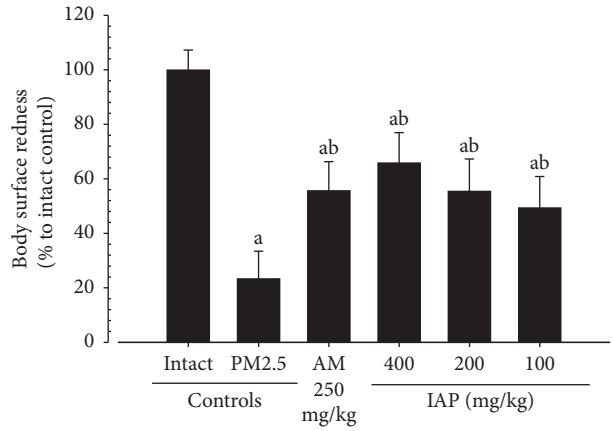


Figure 5: Body surface redness in intact or $PM_{2.5}$-treated pulmonary injured mice. Values are expressed mean ± SD of 10 mice; $PM_{2.5}$ = diesel particulate matter NIST 1650b; AM = ambroxol hydrochloride; IAP = immature Asian pear (fruit of *Pyrus pyrifolia* Nakai cv. Shingo) extract; THSD = Tukey's honest significant difference; [a] $p < 0.01$ as compared with intact vehicle control by THSD test; [b] $p < 0.01$ as compared with $PM_{2.5}$ control by THSD test.

Table 2: Lung weights and goss inspections in intact or $PM_{2.5}$-treated pulmonary injured mice.

| Groups | Lung weights Items (unit) | | Congestional regions (%)-gross findings |
|---|---|---|---|
| | Absolute (g) | Relative (%) | |
| Controls | | | |
| Intact vehicle | 0.117 ± 0.004 | 0.574 ± 0.025 | 1.67 ± 1.50 |
| $PM_{2.5}$ | 0.189 ± 0.020[a] | 0.913 ± 0.107[a] | 57.58 ± 11.20[a] |
| Reference-AM | | | |
| 250 mg/kg | 0.152 ± 0.008[ab] | 0.741 ± 0.035[ab] | 24.73 ± 11.43[ab] |
| Test substance-IAP | | | |
| 400 mg/kg | 0.137 ± 0.010[ab] | 0.671 ± 0.048[ab] | 14.50 ± 4.42[ab] |
| 200 mg/kg | 0.152 ± 0.008[ab] | 0.743 ± 0.033[ab] | 24.82 ± 10.38[ab] |
| 100 mg/kg | 0.160 ± 0.005[ac] | 0.784 ± 0.058[a] | 34.96 ± 10.23[ab] |

Values are expressed mean ± SD of 10 mice; $PM_{2.5}$ = diesel particulate matter NIST 1650b; AM = ambroxol hydrochloride; IAP = immature Asian pear (fruit of *Pyrus pyrifolia* Nakai cv. Shingo) extract; DT3 = Dunnett's T3; [a] $p < 0.01$ as compared with intact vehicle control by DT3 test; [b] $p < 0.01$ and [c] $p < 0.05$ as compared with $PM_{2.5}$ control by DT3 test.

more effective in improving respiratory function. For the experimental results, a representative sample of sputum was compared with that of group 3 [22–25, 29].

Under the conditions of this experiment, no significant changes in body weight and the body weight gain were observed in any of the $PM_{2.5}$-induced lung injury experimental groups compared with those in group 1. No significant changes in body weight and the weight gain were observed in groups 3, 4, 5, and 6 compared with those in group 2. Thus, it can be concluded that, similar to group 1, groups 3, 4, 5, and 6 showed weight changes within the weight gain range of BALB/c mice [52, 65] of the same age.

Expectorants promote mucous secretion in the body, relieve clumped sputum, act as lubricants against airway irritants, and are used in the treatment of various respiratory systems [26]. The expectorant effect has been evaluated based on mucus secretion using various methods, among which the pH-sensitive phenol red tracheal secretion measurement method is the most commonly used [20, 22–25]. This experiment revealed a significant increase in phenol red secretion in TLF in group 2 compared with that in group 1. In addition, a significant increase in organ phenol red secretion was also observed in a dose-dependent manner in groups 4, 5, and 6 compared with that in group 2. In particular, group 5 exhibited an increase in phenol red secretion in TLF that was comparable with that of group 3.

Phenol red is a representative pH-sensitive dye that reacts with alkalis at high pH. During the reaction, it changes color from yellow to red; therefore, it has been used as a pH indicator in various organisms [53, 55]. In individuals with respiratory disorders, the concentration of carbon dioxide increases, and the formation of carbonic acid causes respiratory acidosis, resulting in a drop in pH [25, 66–68]. The results of this experiment showed that body surface redness was significantly reduced in group 2 compared with that in group 1 after intraperitoneal administration of phenol red in group 2, indicating respiratory acidosis due to respiratory failure caused by $PM_{2.5}$. In contrast, a significant increase in body surface redness was observed in a dose-dependent manner in groups 4, 5, and 6 compared with that

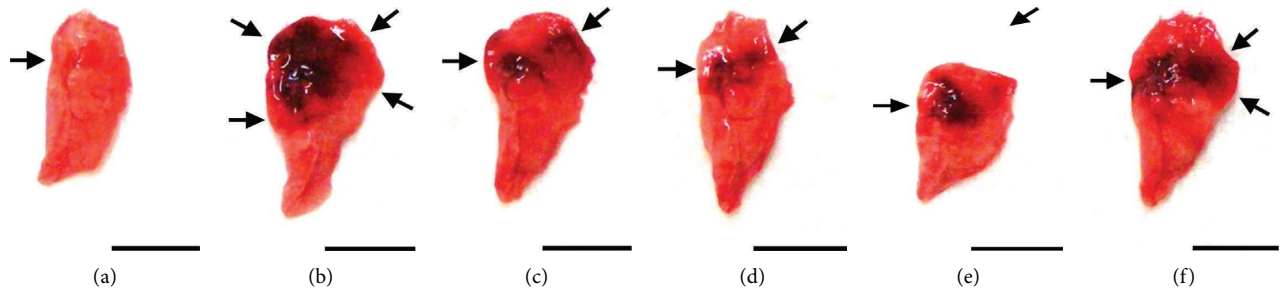


Figure 6: Representative gross lungleft lobe images, taken from Intact or $PM_{2.5}$-treated pulmonary injured mice. (a) = Intact vehicle control (distilled water orally administered mice with saline intranasal instillation); (b) = $PM_{2.5}$ control (distilled water orally administered mice with $PM_{2.5}$ intranasal instillation); (c) = AM250 (250 mg/kg of AM orally administered mice with $PM_{2.5}$ intranasal instillation); (d) = IAP200 (200 mg/kg of IAP orally administered mice with $PM_{2.5}$ intranasal instillation); (e) = IAP100 (100 mg/kg of IAP orally administered mice with $PM_{2.5}$ intranasal instillation); (f) = IAP50 (50 mg/kg of IAP orally administered mice with $PM_{2.5}$ intranasal instillation); $PM_{2.5}$ = diesel particulate matter NIST 1650b; AM = ambroxol hydrochloride; IAP = immature Asian pear (fruit of *Pyrus pyrifolia* Nakai cv. Shingo) extract; arrows indicated congestional regions; scale bars = 6.00 mm.

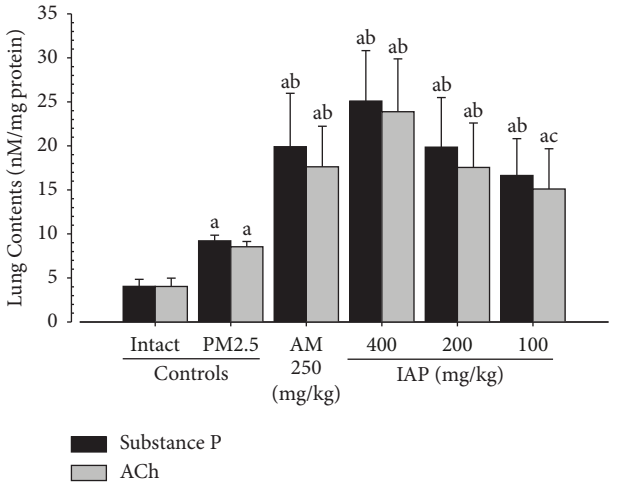


Figure 7: Lung substance P and ACh contents in intact or $PM_{2.5}$-treated pulmonary injured mice. Values are expressed mean ± SD of 10 mice; $PM_{2.5}$ = diesel particulate matter NIST 1650b; AM = ambroxol hydrochloride; IAP = immature Asian pear (fruit of *Pyrus pyrifolia* Nakai cv. Shingo) extract; ACh = acetylcholine; DT3 = Dunnett's T3; $^{a}p < 0.01$ as compared with intact vehicle control by DT3 test; $^{b}p < 0.01$ and $^{c}p < 0.05$ as compared with $PM_{2.5}$ control by DT3 test.

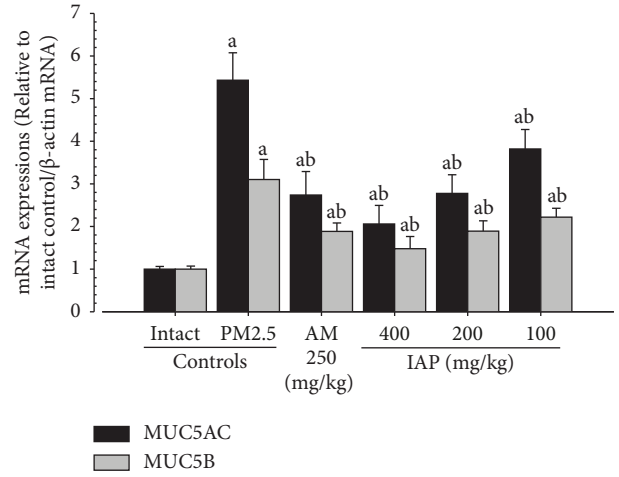


Figure 8: Lung MUC5AC and MUC5B mRNA expressions in intact or $PM_{2.5}$-treated pulmonary injured mice. Values are expressed mean ± SD of 10 mice; $PM_{2.5}$ = diesel particulate matter NIST 1650b; AM = ambroxol hydrochloride; IAP = immature Asian pear (fruit of *Pyrus pyrifolia* Nakai cv. Shingo) extract; MUC = mucin; DT3 = Dunnett's T3; $^{a}p < 0.01$ as compared with intact vehicle control by DT3 test; $^{b}p < 0.01$ as compared with $PM_{2.5}$ control by DT3 test.

in group 2. In particular, group 5 exhibited an inhibitory effect on body surface redness caused by $PM_{2.5}$ comparable with that of group 3. These results provide clear evidence that oral administration of 400, 200, and 100 mg/kg of IAP can inhibit $PM_{2.5}$ respiratory acidosis in a dose-dependent manner through mucolytic expectorant activity. Moreover, the efficacy of 200 mg/kg of IAP is comparable with that of 250 mg/kg of AM.

The mucus present on the surface of the respiratory system plays a crucial role in defense against various infectious agents and foreign substances. Mucin is a glycoprotein component of mucus [69, 70]. The amount and viscosity of mucus in the respiratory system are directly related to the cleansing action of the microcilia. The presence of a large amount of mucus with high viscosity indicates that the cleaning action of the respiratory system via microciliary movement is impaired [59]. MUC5AC and MUC5B are the most common macromolecular substances that constitute the mucus secreted in the respiratory tract [25, 69, 70]. Changes in the expression of MUC5AC and MUC5B are induced in various respiratory diseases [71–73]. In particular, $PM_{2.5}$, which promotes mucus production by increasing the expression of MUC5AC and MUC5B mRNA, forms high-viscosity sputum [25, 69, 70]. In contrast, glandular fluid secretion in the respiratory system is mainly regulated through innervation [74]. Stimulation/excitation of the vagus nervous system results in the local secretion of ACh and large amounts of glandular fluid [75]. Substance P is a representative glandular fluid secretion-promoting factor in the respiratory system [76–78]. The secretion of

Table 3: General histomorphometrical analysis of lung-left lobe tissue in intact or $PM_{2.5}$-treated pulmonary injured mice.

| Groups | Items (unit) | | | | |
|---|---|---|---|---|---|
| | Mean ASA (%/mm$^2$) | Mean alveolar septal thickness ($\mu$m) | Mean thickness of SB ($\mu$m) | Mean IF cell numbers infiltrated in AR (cells/mm$^2$) | PAS-positive cells on the SB (cells/mm$^2$) |
| Controls | | | | | |
| Intact vehicle | 84.38 ± 10.03 | 7.12 ± 1.99 | 16.21 ± 2.19 | 42.00 ± 14.91 | 20.80 ± 4.24 |
| $PM_{2.5}$ | 29.87 ± 10.46[a] | 42.52 ± 5.51[c] | 22.51 ± 1.42[c] | 806.80 ± 110.36[c] | 35.00 ± 4.14[c] |
| Reference-AM | | | | | |
| 250 mg/kg | 61.11 ± 7.40[ab] | 26.51 ± 5.15[cd] | 30.15 ± 2.90[cd] | 298.00 ± 104.86[cd] | 78.60 ± 15.86[cd] |
| Test substance-IAP | | | | | |
| 400 mg/kg | 69.89 ± 7.67[ab] | 20.44 ± 6.66[cd] | 36.37 ± 4.66[cd] | 166.10 ± 59.15[cd] | 96.80 ± 17.99[cd] |
| 200 mg/kg | 61.34 ± 10.01[ab] | 26.52 ± 4.76[cd] | 30.49 ± 3.86[cd] | 297.40 ± 102.48[cd] | 78.30 ± 10.65[cd] |
| 100 mg/kg | 52.70 ± 6.39[ab] | 32.06 ± 2.43[cd] | 27.38 ± 1.46[cd] | 407.90 ± 101.56[cd] | 61.20 ± 14.24[cd] |

Values are expressed as Mean ± SD of 10 mice; $PM_{2.5}$ = diesel particulate matter NIST 1650b; AM = ambroxol hydrochloride; IAP = immature Asian pear (fruit of *Pyrus pyrifolia* Nakai cv. Shingo) extract; ASA = alveolar surface area; SB = secondary bronchus mucosa; IF = Inflammatory; AR = alveolar region; PAS = periodic acid Schiff; THSD = Tukey's honest significant difference; DT3 = Dunnett's T3; [a]$p < 0.01$ as compared with intact vehicle control by THSD test; [b]$p < 0.01$ as compared with $PM_{2.5}$ control by THSD test; [c]$p < 0.01$ as compared with intact vehicle control by DT3 test; [d]$p < 0.01$ as compared with $PM_{2.5}$ control by DT3 test.

glandular fluid in the respiratory system is mainly regulated by ACh and substance P [74, 75]. In contrast, substance P also acts as a neurogenic inflammatory factor in the respiratory system [79], and it is known that $PM_{2.5}$ treatment induces a significant increase in substance P as a neurogenic inflammatory factor [25, 59, 80]. The treatment of $PM_{2.5}$-induced damage is also associated with an increase in vascular permeability [2, 3, 25], a part of an inflammatory response, resulting in an increase in the ACh content as a vasorelaxant factor [81]. However, vascular reactivity to ACh is significantly reduced in mice with $PM_{2.5}$-induced lung injury [25, 82].

As part of a prominent neurogenic inflammatory response in lung tissue, the production of high-viscosity mucus was induced by increased MUC5AC and MUC5B mRNA expression [25, 69, 70] along with an increase in the ACh and substance P content [25, 59, 80–82] in group 2 compared with that in group 1 in this study. Meanwhile, as part of the mucolytic expectorant activity, significant increases in the content of substances P and ACh, which promote glandular fluid production [74, 75], and decreases in mucus production-related genes MUC5AC and MUC5B mRNA [25, 69, 70], were observed in a dose-dependent manner in groups 4, 5, and 6 compared with those in group 2. In particular, group 5 exhibited increased substance P and Ach content in lung tissue and decreased mRNA expression of mucus production-related genes MUC5AC and MUC5B compared with that in group 3 in the $PM_{2.5}$-induced subacute lung injury Balb/c mouse model. These results provide clear evidence that oral administration of 400, 200, and 100 mg/kg of IAP resulted in mucolytic expectorant activity in the $PM_{2.5}$-induced lung injury in the Balb/c mouse model through the promotion of glandular fluid production by increasing the production of substances P and ACh and the reduction of mucin through the reduction of MUC5AC and MUC5B mRNA expression. The effects of 200 mg/kg of IAP were comparable with those of 250 mg/kg of AM.

Lung weight, which is relative to body weight, has been used as an important indicator for evaluating pulmonary edema due to increased vascular leakage [25, 48, 83]. Similar to the ovalbumin-induced asthma model [60, 84] that also used mice with $PM_{2.5}$ inhalation, vascular leakage was found to increase through the weakening of the binding force of vascular endothelial cells due to the inflammatory response, resulting in pulmonary edema [2, 3, 25]. Intranasal injection of $PM_{2.5}$ results in lung enlargement with significant local congestion. Pulmonary edema and significant increases in the area of gross congestion and absolute and relative lung weights were observed compared with those in group 1. However, significant reductions in gross congestion in the lungs and absolute and relative weights were observed in a dose-dependent manner in groups 4, 5, and 6 compared with those in group 2. In particular, group 5 exhibited consistent suppression of $PM_{2.5}$-induced pulmonary congestion; enlargement; and an increase in absolute and relative weight comparable with those of group 3. These results provide reliable evidence that $PM_{2.5}$-induced pulmonary edema is significantly suppressed in a dose-dependent manner by the oral administration of 400, 200, and 100 mg/kg of IAP. The effects of 200 mg/kg of IAP were comparable with those of 250 mg/kg of AM.

Histomorphometrically, ASA (%/mm$^2$) has been used as an indirect indicator of the gas exchange capacity of the lungs. A decrease in ASA indicates a decrease in the gas exchange surface area of the lung, that is, a decrease in lung function. A decrease in ASA has been observed in various lung diseases [22–25, 47, 48, 85, 86]. PAS staining is a traditional histochemical staining method that has been used to specifically stain mucus-secreting cells. An increase in PAS staining indicates an increase in the activity of mucus-producing cells [87]. An increase in the number of PAS-positive mucus-producing cells in the bronchial mucosa, along with bronchial mucosal thickening, has an expectorant effect histopathologically [20, 22–25]. Apoptosis is an important regulator of cell death.

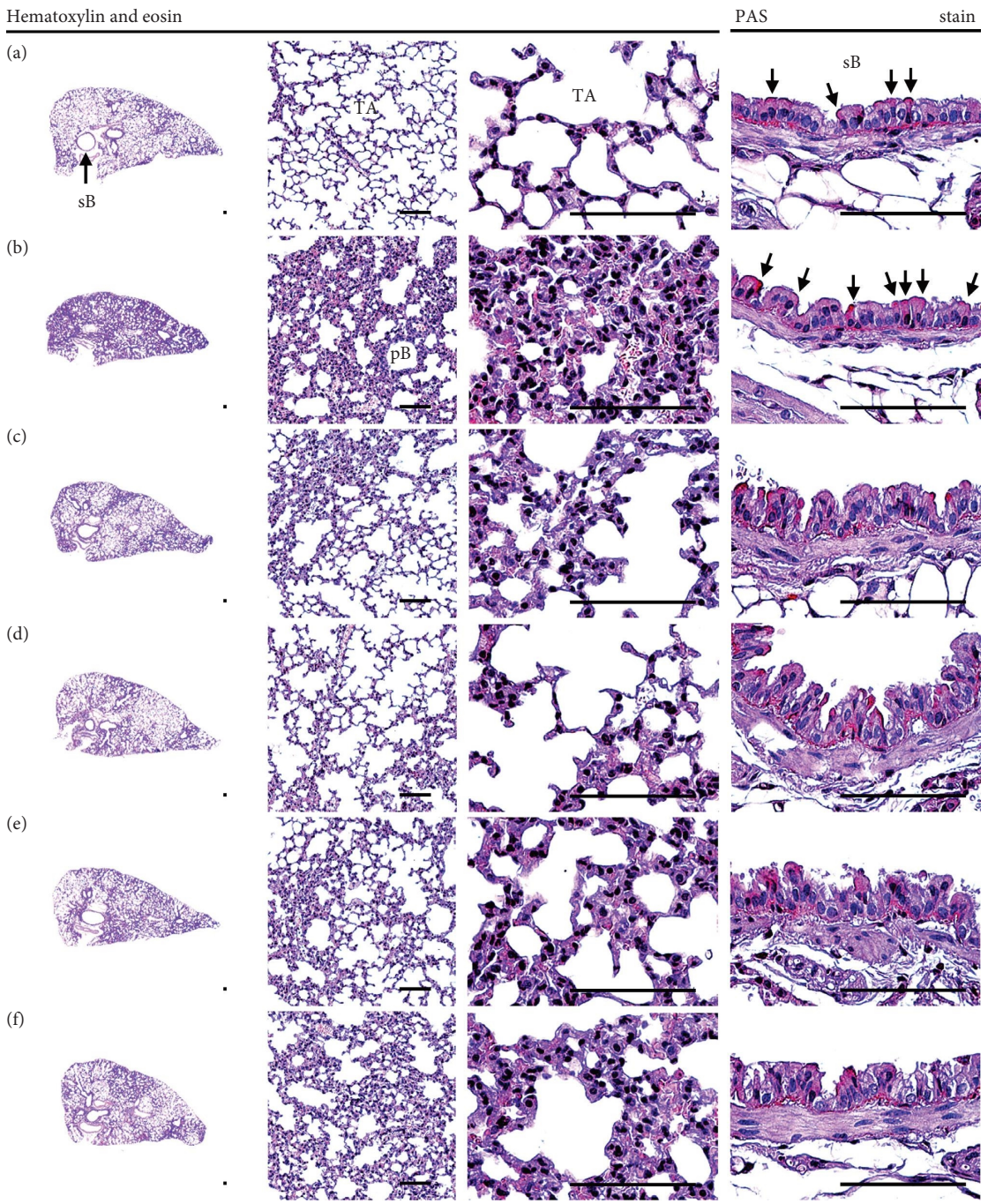


Figure 9: Representative general histopathological profiles of the lung-left lobe tissues, taken from intact or $PM_{2.5}$-treated pulmonary injured mice. (a) Intact vehicle control (distilled water orally administered mice with saline intranasal instillation); (b) $PM_{2.5}$ control (distilled water orally administered mice with $PM_{2.5}$ intranasal instillation); (c) AM250 (250 mg/kg of AM orally administered mice with $PM_{2.5}$ intranasal instillation); (d) IAP200 (200 mg/kg of IAP orally administered mice with $PM_{2.5}$ intranasal instillation); (e) IAP100 (100 mg/kg of IAP orally administered mice with $PM_{2.5}$ intranasal instillation); (f) IAP50 (50 mg/kg of IAP orally administered mice with $PM_{2.5}$ intranasal instillation); $PM_{2.5}$ = diesel particulate matter NIST 1650b; AM = ambroxol hydrochloride; IAP = immature Asian pear (fruit of *Pyrus pyrifolia* Nakai cv. Shingo) extract; ASA = alveolar surface area; PAS = periodic acid Schiff; sB = secondary bronchus; pB = primary bronchiole; TA = terminal respiratory bronchiole-alveoli; arrows indicated PAS-positive mucus producing cells; scale bars = 200 $\mu$m.

Apoptotic cells are characterized by chromatin enrichment and the formation of apoptotic bodies [88, 89] by the activation of cleaved caspase-3 [90, 91], a representative apoptosis marker. Oxidative stress caused by $PM_{2.5}$ induces mitochondria-dependent apoptosis [92]. Therefore, the increase in cleaved caspase-3 in lung parenchymal cells

Table 4: Immunohistochemistrical stain-based histomorphometrical analysis of lung-left lobe tissue in intact or $PM_{2.5}$-treated pulmonary injured mice.

| Groups | Items/regions | | | |
|---|---|---|---|---|
| | Caspase-3 immunolabeled cells | | COX-2 immunostained cells | |
| | AR region | SB mucosa region | AR region | SB mucosa region |
| Controls | | | | |
| Intact vehicle | 40.40 ± 12.89 | 11.20 ± 4.02 | 48.20 ± 14.71 | 19.60 ± 5.64 |
| $PM_{2.5}$ | 386.60 ± 77.52[a] | 274.60 ± 64.49[a] | 489.60 ± 114.10[a] | 164.60 ± 27.11[a] |
| Reference-AM | | | | |
| 250 mg/kg | 147.20 ± 32.72[ab] | 74.40 ± 21.04[ab] | 216.60 ± 49.92[ab] | 67.00 ± 20.25[ab] |
| Test substance-IAP | | | | |
| 400 mg/kg | 95.60 ± 16.43[ab] | 40.00 ± 11.16[ab] | 113.40 ± 26.70[ab] | 31.40 ± 12.37[b] |
| 200 mg/kg | 143.60 ± 30.09[ab] | 74.20 ± 18.72[ab] | 215.20 ± 40.76[ab] | 69.40 ± 21.48[ab] |
| 100 mg/kg | 203.60 ± 38.25[ab] | 185.40 ± 10.83[ac] | 307.60 ± 32.32[ab] | 104.00 ± 10.54[ab] |

Values are expressed mean ± SD of 10 mice; cells/$mm^2$; $PM_{2.5}$ = diesel particulate matter NIST 1650b; AM = ambroxol hydrochloride; IAP = immature Asian pear (fruit of *Pyrus pyrifolia* Nakai cv. Shingo) extract; COX = cyclooxygenase; AR = alveolar septal; SB = secondary bronchus mucosa; DT3 = Dunnett's T3; [a]$p < 0.01$ as compared with intact vehicle control by DT3 test; [b]$p < 0.01$ and [c]$p < 0.05$ as compared with $PM_{2.5}$ control by DT3 test.

following exposure to $PM_{2.5}$ indicates cell damage by apoptosis [25, 70]. COX-2 is an important enzyme involved in the synthesis of prostaglandin, a chemical mediator of inflammation, and is known to be involved in angiogenesis and the progression of inflammation [93, 94]. Significant increases in COX-2 occur during $PM_{2.5}$-induced lung injury [25, 95, 96]. At present, the suppression of COX-2 immunoreactivity is used as an important index for evaluating anti-inflammatory effects [97, 98]. Similar to the histopathological results of drug efficacy experiments in the previous $PM_{2.5}$-induced lung injury model [2, 3, 12, 25], histopathologically significant sarcoma lesions (alveolar septum thickening due to inflammatory cell infiltration, secondary bronchial mucosal thickening, and PAS-positive mucus-producing cells increase) were observed following intranasal injection of 1 mg/kg $PM_{2.5}$ in this study.

We observed a significant increase in the average alveolar septal and secondary bronchial mucosal thickness, the number of inflammatory cells infiltrating around the alveoli, and the number of PAS-positive mucus-producing cells in the secondary bronchial mucosa. A decrease in ASA was associated with this. An increased number of secondary bronchial mucosal cleaved caspase-3 and COX-2 immunoreactive cells was observed compared with that in group 1. However, at all three doses of IAP (400, 200, and 100 mg/kg), significant increases in ASA, mean alveolar septum thickness, and the number of infiltrating inflammatory cells around the alveoli and alveolar septum, as well as a decrease in the number of secondary bronchial mucosal apoptosis-related cleaved caspase-3 and inflammation-related COX-2 immune response cells were observed in a dose-dependent manner in groups 4, 5, and 6 compared with those in group 2. In particular, group 5 exhibited a reduction in $PM_{2.5}$-induced alveolar septal thickening and inflammatory cell infiltration, and the associated ASA and secondary bronchial mucosal cleaved caspase-3 and COX-2 immunoreactive cells were shown to inhibit the increase in the number. These effects were comparable with those of group 3. In addition, as part of the expectorant activity [20, 22–25], significant increases in the mean thickness of secondary bronchial mucosa and the number of PAS-positive mucus-producing cells were observed in groups 4, 5, and 6 compared with those in group 2. In particular, secondary bronchial mucosal thickness and the number of PAS-positive mucus-producing cells increased in group 5 in a manner comparable with that of group 3.

These results reliably indicate that oral administration of IAP at doses of 400, 200, and 100 mg/kg inhibited $PM_{2.5}$-induced inflammatory lung damage in a dose-dependent manner through expectorant and anti-inflammatory activities, which was comparable with the effects of an oral dose of 250 mg/kg of AM. Thus, oral administration of an appropriate dose of IAP is highly likely to be an effective respiratory function-improving natural drug or health functional food material in the future. However, this study has certain limitations which need to be addressed in the future studies. Further mechanistic investigations, such as signaling pathway analysis or cellular studies, would provide more detailed insights into how the pear extracts exert their specific expectorant effects. While the in vitro and in vivo experimental analyses in this study offer valuable insights, they may not fully replicate the complexity of human respiratory conditions. Therefore, caution should be exercised when extrapolating the findings to clinical scenarios. Nevertheless, this study focuses on the specific expectorant effects of the pear extracts and their potential implications in addressing $PM_{2.5}$-induced respiratory issues; further research should investigate the broader effects of the pear extracts for other respiratory parameters, such as, lung dysbiosis or lung barrier rainforcement."

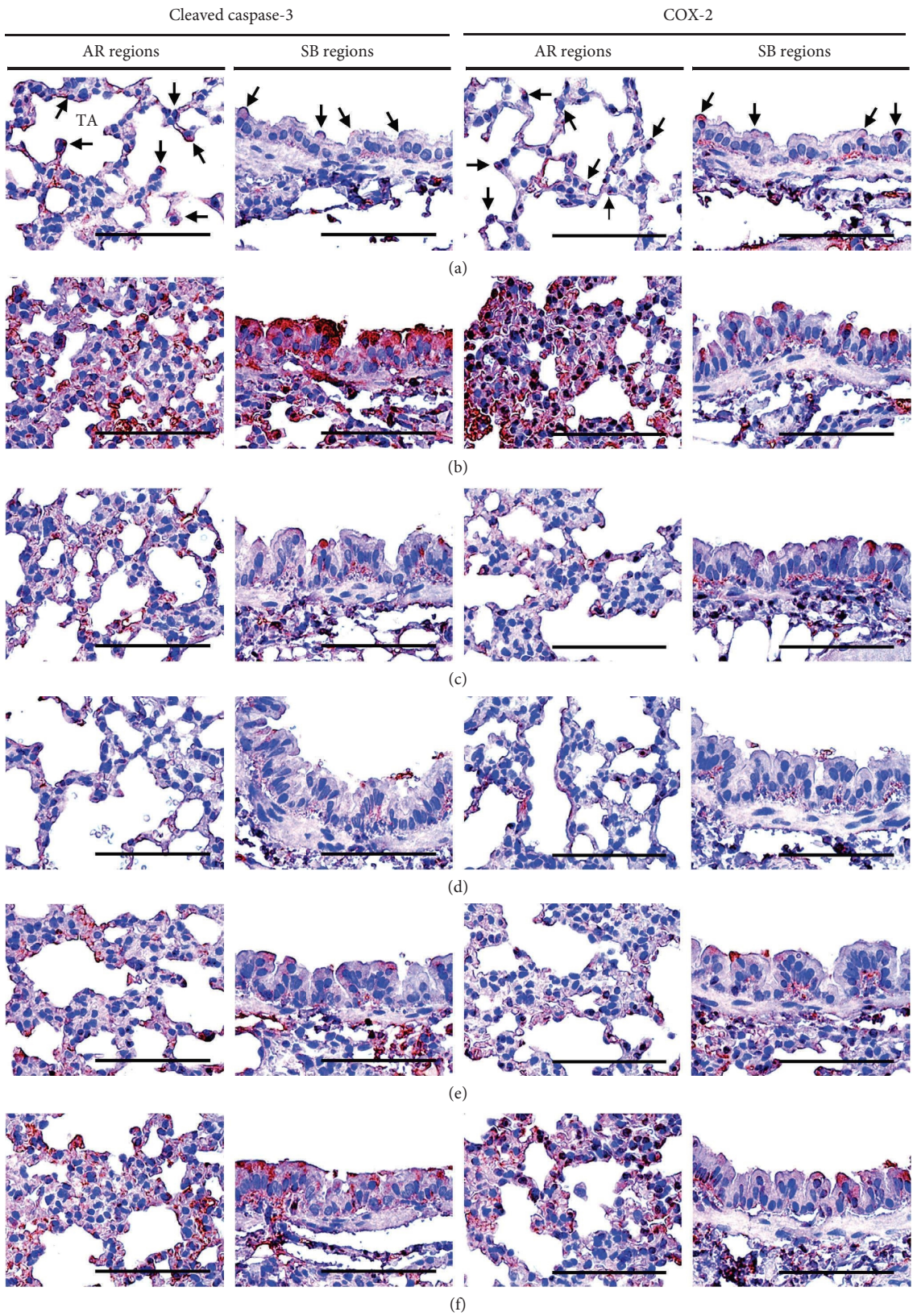


FIGURE 10: Representative immunohistochemistrical stain-based histopathological profiles of the lung-left lobe tissues, taken from intact or $PM_{2.5}$-treated pulmonary injured mice. (a) Intact vehicle control (distilled water orally administered mice with saline intranasal instillation); (b) $PM_{2.5}$ control (distilled water orally administered mice with $PM_{2.5}$ intranasal instillation); (c) AM250 (250 mg/kg of AM orally administered mice with $PM_{2.5}$ intranasal instillation); (d) IAP200 (200 mg/kg of IAP orally administered mice with $PM_{2.5}$ intranasal instillation); (e) IAP100 (100 mg/kg of IAP orally administered mice with $PM_{2.5}$ intranasal instillation); (f) IAP50 (50 mg/kg of IAP orally administered mice with $PM_{2.5}$ intranasal instillation); $PM_{2.5}$ = diesel particulate matter NIST 1650b; AM = ambroxol hydrochloride; IAP = immature Asian pear (fruit of *Pyrus pyrifolia* Nakai cv. Shingo) extract; AR = alveolar septal; SB = secondary bronchus mucosa; COX = cyclooxygenase; ABC = avidin-biotin-peroxidase complex; sB = secondary bronchus; TA = terminal respiratory bronchiole-alveoli; arrows indicated immunoreactive cells; all ABC based immunohistochemistrical stain; scale bars = 200 $\mu$m.

## 6. Conclusion

The results of this experiment show that $PM_{2.5}$-induced inflammatory lung damage, increased sputum, associated respiratory acidosis were significantly suppressed in a dose-dependent manner by the administration of 400, 200, and 100 mg/kg of IAP, and the effects of IAP (200 mg/kg) administration were comparable with those of 250 mg/kg of AM. As part of the mucolytic expectorant activity, significant pH-sensitivity, phenol red secretion in the trachea, substance P and Ach content promoting glandular fluid production in lung tissue, and an increase in the average thickness of secondary bronchial mucosa were observed. The number of PAS-positive mucus-producing cells increased and decreased in mucus-production-related genes. MUC5AC and MUC5B mRNA expression were also observed in all three doses of IAP administration. Moreover, the effects were comparable with those of 250 mg/kg of AM at a dose of 200 mg/kg. These results are considered reliable evidence and indicate that oral administration of 400, 200, and 100 mg/kg of IAP inhibits $PM_{2.5}$-induced inflammatory lung damage and increases sputum and associated respiratory acidosis, along with anti-inflammatory activity, through mucolytic expectorant activity through increased production of substance P and ACh, and decreased expression of MUC5AC and MUC5B mRNA in a dose-dependent manner, as compared with the AM (250 mg/kg) administered group. This study shows that oral administration of an appropriate dose of IAP is highly likely to be an effective natural drug or functional food material for improving respiratory function in the future.

## Data Availability

The data used to support the findings of this study are available from the corresponding author upon request.

## Conflicts of Interest

The authors declare that there are no conflicts of interest regarding the publication of this article.

## Authors' Contributions

Bertoka Fajar Surya Perwira Negara and Joo Wan Kim contributed equally to this study.

## Acknowledgments

This study was supported by the Korea Institute of Planning and Evaluation for Technology in Food, Agriculture, Forestry (IPET) through High Value-added Food Technology Development Program, funded by the Ministry of Agriculture, Food and Rural Affairs (MAFRA) (grant no. 122027-2).

## References

[1] I. S. Fernando, T. U. Jayawardena, H. S. Kim et al., "Beijing urban particulate matter-induced injury and inflammation in human lung epithelial cells and the protective effects of fucosterol from *Sargassum binder*i (Sonder ex J. Agardh)," *Environmental Research*, vol. 172, pp. 150–158, 2019.

[2] W. Lee, S. K. Ku, J. E. Kim, S. H. Cho, G. Y. Song, and J. S. Bae, "Inhibitory effects of protopanaxatriol type ginsenoside fraction (Rgx365) on particulate matter-induced pulmonary injury," *Journal of Toxicology and Environmental Health, Part A*, vol. 82, no. 5, pp. 338–350, 2019.

[3] W. Lee, S. K. Ku, J. E. Kim, S. H. Cho, G. Y. Song, and J. S. Bae, "Inhibitory effects of black ginseng on particulate matter-induced pulmonary injury," *The American Journal of Chinese Medicine*, vol. 47, no. 06, pp. 1237–1251, 2019.

[4] G. Zhuang, J. Guo, H. Yuan, and C. Zhao, "The compositions, sources, and size distribution of the dust storm from China in spring of 2000 and its impact on the global environment," *Chinese Science Bulletin*, vol. 46, no. 11, pp. 895–900, 2001.

[5] W. Wang, T. Primbs, S. Tao, and S. L. Simonich, "Atmospheric particulate matter pollution during the 2008 Beijing Olympics," *Environmental Science and Technology*, vol. 43, no. 16, pp. 6440–5320, 2009.

[6] X. F. Huang, L. Y. He, M. Hu, and Y. H. Zhang, "Annual variation of particulate organic compounds in $PM_{2.5}$ in the urban atmosphere of Beijing," *Atmospheric Environment*, vol. 40, no. 14, pp. 2449–2458, 2006.

[7] C. Nunes, A. M. Pereira, and M. Morais-Almeida, "Asthma costs and social impact," *Asthma Research and Practice*, vol. 3, no. 1, 2017.

[8] H. F. Chiu, S. S. Tsai, and C. Y. Yang, "Short-term effects of fine particulate air pollution on hospital admissions for hypertension: a time-stratified case-crossover study in Taipei," *Journal of Toxicology and Environmental Health, Part A*, vol. 80, no. 5, pp. 258–265, 2017.

[9] World Health Organization, "Air pollution," 2023, https://www.who.int/health-topics/air-pollution#tab=tab_1.

[10] G. Wang, L. Huang, S. Gao, S. Gao, and L. Wang, "Measurements of $PM_{10}$ and $PM_{2.5}$ in urban area of Nanjing, China and the assessment of pulmonary deposition of particle mass," *Chemosphere*, vol. 48, no. 7, pp. 689–695, 2002.

[11] R. Pozzi, B. De Berardis, L. Paoletti, and C. Guastadisegni, "Inflammatory mediators induced by coarse ($PM_{2.5-10}$) and fine ($PM_{2.5}$) urban air particles in RAW 264.7 cells," *Toxicology*, vol. 183, no. 1-3, pp. 243–254, 2003.

[12] F. Wang, R. Wang, and H. Liu, "The acute pulmonary toxicity in mice induced by *Staphylococcus aureus*, particulate matter, and their combination," *Experimental Animals*, vol. 68, no. 2, pp. 159–168, 2019.

[13] A. H. Morice, G. A. Fontana, M. G. Belvisi et al., "ERS guidelines on the assessment of cough," *European Respiratory Journal*, vol. 29, no. 6, pp. 1256–1276, 2007.

[14] S. S. Birring, B. Prudon, A. J. Carr, S. J. Singh, M. D. L. Morgan, and I. D. Pavord, "Development of a symptom specific health status measure for patients with chronic cough Leicester Cough Questionnaire (LCQ)," *Thorax*, vol. 58, no. 4, pp. 339–343, 2003.

[15] I. D. Pavord, "Cough and asthma," *Pulmonary Pharmacology & Therapeutics*, vol. 17, no. 6, pp. 399–402, 2004.

[16] G. Dapaah, G. A. Koffuor, P. K. Mante, and I. O. Ben, "Antitussive, expectorant and analgesic effects of the ethanol seed extract of *Picralima nitida* (Stapf) Th. & H. Durand," *Research in Pharmaceutical Sciences*, vol. 11, no. 2, pp. 100–112, 2016.

[17] P. V. Dicpinigaitis and Y. E. Gayle, "Effect of guaifenesin on cough reflex sensitivity," *Chest*, vol. 124, no. 6, pp. 2178–2181, 2003.

[18] M. Sanak, "Eicosanoid mediators in the airway inflammation of asthmatic patients: what is new?" *Allergy, Asthma & Immunology Research*, vol. 8, no. 6, pp. 481–490, 2016.

[19] J. R. Woloski, S. Heston, and S. P. Escobedo Calderon, "Respiratory allergic disorders," *Primary Care: Clinics in Office Practice*, vol. 43, no. 3, pp. 401–415, 2016.

[20] D. Wang, S. Wang, X. Chen et al., "Antitussive, expectorant and anti-inflammatory activities of four alkaloids isolated from Bulbus of *Fritillaria wabuensis*," *Journal of Ethnopharmacology*, vol. 139, no. 1, pp. 189–193, 2012.

[21] P. Yu, S. Cheng, J. Xiang et al., "Expectorant, antitussive, anti-inflammatory activities and compositional analysis of *Aster tataricus*," *Journal of Ethnopharmacology*, vol. 164, pp. 328–333, 2015.

[22] J.-R. Hu, C.-J. Jung, S.-M. Ku, D.-H. Jung, S.-K. Ku, and J.-S. Choi, "Antitussive, expectorant, and anti-inflammatory effects of Adenophorae Radix powder in ICR mice," *Journal of Ethnopharmacology*, vol. 239, Article ID 111915, 2019.

[23] J.-R. Hu, C.-J. Jung, S.-M. Ku et al., "Anti-inflammatory, expectorant, and antitussive properties of Kyeongok-go in ICR mice," *Pharmaceutical Biology*, vol. 59, no. 1, pp. 319–332, 2021.

[24] J.-R. Hu, C.-J. Jung, S.-M. Ku et al., "Deciphering the antitussive, expectorant, and anti-inflammatory potentials of ShashamKyeongok-Go and their phytochemical attributes: in vivo appraisal in ICR mice," *Applied Sciences*, vol. 11, no. 3, p. 1349, 2021.

[25] S.-M. Park, C.-J. Jung, D.-G. Lee et al., "Adenophora stricta root extract protects lung injury from exposure to particulate matter 2.5 in mice," *Antioxidants*, vol. 11, no. 7, p. 1376, 2022.

[26] A. G. G. Garay, L. Reveiz, H. L. Velasco, and G. C. Solis, "Ambroxol for women at risk of preterm birth for preventing neonatal respiratory distress syndrome," *Cochrane Database of Systematic Reviews*, vol. 10, 2014.

[27] B. K. Rubin, "Aerosol medications for treatment of mucus clearance disorders," *Respiratory Care*, vol. 60, no. 6, pp. 825–832, 2015.

[28] K. M. Beeh, J. Beier, A. Esperester, and L. D. Paul, "Anti-inflammatory properties of ambroxol," *European Journal of Medical Research*, vol. 13, no. 12, pp. 557–562, 2008.

[29] M. Malerba and B. Ragnoli, "Ambroxol in the 21st century: pharmacological and clinical update," *Expert Opinion on Drug Metabolism and Toxicology*, vol. 4, no. 8, pp. 1119–1129, 2008.

[30] D. Paleari, G. A. Rossi, G. Nicolini, and D. Olivieri, "Ambroxol: a multifaceted molecule with additional therapeutic potentials in respiratory disorders of childhood," *Expert Opinion on Drug Discovery*, vol. 6, no. 11, pp. 1203–1214, 2011.

[31] G. Molina, E. Holguin, and E. Teran, "Oral ambroxol supplement in pregnant women induces fetal lung maturation," *American Journal of Obstetrics and Gynecology*, vol. 191, no. 6, p. 2177, 2004.

[32] H.-S. Kim, S.-I. Park, S.-H. Choi et al., "Single oral dose toxicity test of blue honeysuckle concentrate in mice," *Toxicological Research*, vol. 31, no. 1, pp. 61–68, 2015.

[33] L. Z. Lin and J. M. Harnly, "Phenolic compounds and chromatographic profiles of pear skins (*Pyrus* spp.)," *Journal of Agricultural and Food Chemistry*, vol. 56, no. 19, pp. 9094–9101, 2008.

[34] D. Tanrioven and A. Eksi, "Phenolic compounds in pear juice from different cultivars," *Food Chemistry*, vol. 93, no. 1, pp. 89–93, 2005.

[35] S.-W. Lee, J.-Y. Cho, H.-Y. Jeong, T.-W. Na, S.-H. Lee, and J.-H. Moon, "Enhancement of antioxidative and antimicrobial activities of immature pear (*Pyrus pyrifolia* cv. Niitaka) fruits by fermentation with *Leuconostoc mesenteroides*," *Food Science and Biotechnology*, vol. 25, no. 6, pp. 1719–1726, 2016.

[36] J.-Y. Cho, C. M. Kim, H.-J. Lee et al., "Caffeoyl triterpenes from pear (*Pyrus pyrifolia* Nakai) fruit peels and their antioxidative activities against oxidation of rat blood plasma," *Journal of Agricultural and Food Chemistry*, vol. 61, no. 19, pp. 4563–4569, 2013.

[37] K.-H. Lee, J.-Y. Cho, H.-J. Lee et al., "Hydroxycinnamoylmalic acids and their methyl esters from pear (*Pyrus pyrifolia* Nakai) fruit peel," *Journal of Agricultural and Food Chemistry*, vol. 59, no. 18, pp. 10124–10128, 2011.

[38] H.-S. Lee, T. Isse, T. Kawamoto, H. W. Baik, J. Y. Park, and M. Yang, "Effect of Korean pear (*Pyrus pyrifolia* cv. Shingo) juice on hangover severity following alcohol consumption," *Food and Chemical Toxicology*, vol. 58, pp. 101–106, 2013.

[39] Y. G. Lee, J.-Y. Cho, C.-M. Kim et al., "Isolation and identification of 3 low-molecular compounds from pear (*Pyrus pyrifolia* Nakai cv. Chuhwangbae) fruit peel," *Korean Journal of Food Science and Technology*, vol. 45, no. 2, pp. 174–179, 2013.

[40] J.-Y. Cho, Y. G. Lee, S.-H. Lee, W.-S. Kim, K.-H. Park, and J.-H. Moon, "An ether and three ester derivatives of phenylpropanoid from pear (*Pyrus pyrifolia* Nakai cv. Chuhwangbae) fruit and their radical-scavenging activity," *Food Science and Biotechnology*, vol. 23, no. 1, pp. 253–259, 2014.

[41] J.-Y. Cho, S.-H. Lee, E. H. Kim et al., "Change in chemical constituents and free radical-scavenging activity during pear (*Pyrus pyrifolia*) cultivar fruit development," *Bioscience, Biotechnology, and Biochemistry*, vol. 79, no. 2, pp. 260–270, 2015.

[42] S. W. Lee, Y. G. Lee, J.-Y. Cho et al., "Establishment of a simple method for purification of high purity chlorogenic acid from immature fruit of pear (*Pyrus pyrifolia* Nakai)," *Journal of the Korean Society for Applied Biological Chemistry*, vol. 58, no. 3, pp. 335–341, 2015.

[43] J.-Y. Cho, K. Y. Park, K. H. Lee et al., "Recovery of arbutin in high purity from fruit peels of pear (*Pyrus pyrifolia* Nakai)," *Food Science and Biotechnology*, vol. 20, no. 3, pp. 801–807, 2011.

[44] X. Deng, W. Rui, F. Zhang, and W. Ding, "$PM_{2.5}$ induces Nrf2-mediated defense mechanisms against oxidative stress by activating PIK3/AKT signaling pathway in human lung alveolar epithelial A549 cells," *Cell Biology and Toxicology*, vol. 29, no. 3, pp. 143–157, 2013.

[45] Y. Jin, W. Wu, W. Zhang et al., "Involvement of EGF receptor signaling and NLRP12 inflammasome in fine particulate matter-induced lung inflammation in mice," *Environmental Toxicology*, vol. 32, no. 4, pp. 1121–1134, 2017.

[46] T. D. Schmittgen and K. J. Livak, "Analyzing real-time PCR data by the comparative CT method," *Nature Protocols*, vol. 3, no. 6, pp. 1101–1108, 2008.

[47] S. K. Ku, J. W. Kim, H. R. Cho et al., "Effect of $\beta$-glucan originated from *Aureobasidium pullulans* on asthma induced by ovalbumin in mouse," *Archives of Pharmacal Research*, vol. 35, no. 6, pp. 1073–1081, 2012.

[48] B. G. Min, S. M. Park, Y. W. Choi et al., "Effects of *Pelargonium sidoides* and Coptis Rhizoma 2: 1 mixed formula (PS + CR) on ovalbumin-induced asthma in mice," *Evidence-based Complementary and Alternative Medicine*, vol. 2020, Article ID 9135637, 14 pages, 2020.

[49] D. M. André, C. M. Horimoto, M. C. Calixto, E. C. Alexandre, and E. Antunes, "Epigallocatechin-3-gallate protects against the exacerbation of allergic eosinophilic inflammation

associated with obesity in mice," *International Immunopharmacology*, vol. 62, pp. 212–219, 2018.

[50] C. D. Phung, T. T. Pham, H. T. Nguyen et al., "Anti-CTLA-4 antibody-functionalized dendritic cell-derived exosomes targeting tumor-draining lymph nodes for effective induction of antitumor T-cell responses," *Acta Biomaterialia*, vol. 115, pp. 371–382, 2020.

[51] K. Poudel, S. Park, J. Hwang et al., "Photothermally Modulatable and structurally disintegratable sub-8-nm Au1Ag9 Embedded nanoblocks for combination cancer therapy produced by plug-in assembly," *ACS Nano*, vol. 14, no. 9, Article ID 11040, 2020.

[52] Y. Tajima, *Biological Reference Data Book on Experimental Animals*, Soft Science Inc, Tokyo, Japan, 1989.

[53] P. Rous, "The relative reaction within living mammalian tissues: III. Indicated differences in the reaction of the blood and tissues on vital staining with phthaleins," *Journal of Experimental Medicine*, vol. 41, no. 4, pp. 451–470, 1925.

[54] J. Zhou, L. Han, Y. Ling, L. Wang, N. B. Li, and H. Q. Luo, "A visual detection of human immunodeficiency virus gene using ratiometric method enabled by phenol red and target-induced catalytic hairpin assembly," *Talanta*, vol. 219, Article ID 121202, 2020.

[55] S. Paliwal, V. Sudan, D. Shanker, and M. Srivastava, "Rapid diagnosis of *Theileria annulata* by colorimetric loop-mediated isothermal amplification (LAMP) assay," *Veterinary Parasitology*, vol. 285, Article ID 109224, 2020.

[56] B. Lv, B. Zhang, and Y. Bai, "A systematic analysis of $PM_{2.5}$ in Beijing and its sources from 2000 to 2012," *Atmospheric Environment*, vol. 124, pp. 98–108, 2016.

[57] C. H. Sodikoff, *Laboratory Profiles of Small Animal Diseases, A Guide to Laboratory Diagnosis*, Mosby, St. Louise, MO, United States, 1995.

[58] Y. F. Xing, Y. H. Xu, M. H. Shi, and Y. X. Lian, "The impact of $PM_{2.5}$ on the human respiratory system," *Journal of Thoracic Disease*, vol. 8, no. 1, pp. 69–74, 2016.

[59] H. Liu, X. Fan, N. Wang, Y. Zhang, and J. Yu, "Exacerbating effects of $PM_{2.5}$ in OVA-sensitized and challenged mice and the expression of TRPA1 and TRPV1 proteins in lungs," *Journal of Asthma*, vol. 54, no. 8, pp. 807–817, 2017.

[60] I. Tillie-Leblond, P. Gosset, R. Le Berre et al., "Keratinocyte growth factor improves alterations of lung permeability and bronchial epithelium in allergic rats," *European Respiratory Journal*, vol. 30, no. 1, pp. 31–39, 2007.

[61] T. M. de Kok, L. G. Engels, E. J. Moonen, and J. C. Kleinjans, "Inflammatory bowel disease stimulates formation of carcinogenic N-nitroso compounds," *Gut*, vol. 54, no. 5, p. 731, 2005.

[62] Y. Sun, Y. Yin, J. Zhang et al., "Hydroxyl radical generation and oxidative stress in *Carassius auratus* liver, exposed to pyrene," *Ecotoxicology and Environmental Safety*, vol. 71, no. 2, pp. 446–453, 2008.

[63] S. Wu, F. Deng, Y. Hao et al., "Fine particulate matter, temperature, and lung function in healthy adults: findings from the HVNR study," *Chemosphere*, vol. 108, pp. 168–174, 2014.

[64] C. I. Falcon-Rodriguez, A. R. Osornio-Vargas, I. Sada-Ovalle, P. Segura-Medina, and Aeroparticles, "Aeroparticles, composition, and lung diseases," *Frontiers in Immunology*, vol. 7, p. 3, 2016.

[65] J. G. Fox, B. J. Cohen, and F. M. Loew, *Laboratory Animal Medicine*, Academic Press. Inc, Orlando, FL, USA, 1984.

[66] X. Liu, Y. Jiang, X. Jia et al., "Identification of distinct clinical phenotypes of acute respiratory distress syndrome with differential responses to treatment," *Critical Care*, vol. 25, no. 1, p. 320, 2021.

[67] T. Tonetti, L. Pisani, I. Cavalli et al., "Extracorporeal carbon dioxide removal for treatment of exacerbated chronic obstructive pulmonary disease (ORION): study protocol for a randomised controlled trial," *Trials*, vol. 22, no. 1, p. 718, 2021.

[68] S. Yadav, S. K. Jha, N. Sunuwar, and A. R. Twayana, "Acid-base disorder in the patients visiting the emergency department of a tertiary care hospital: a descriptive cross-sectional study," *Journal of the Nepal Medical Association*, vol. 59, no. 239, pp. 692–696, 2021.

[69] H. G. Na, Y. D. Kim, Y. S. Choi, C. H. Bae, and S. Y. Song, "Diesel exhaust particles elevate MUC5AC and MUC5B expression via the TLR4-mediated activation of ERK1/2, p38 MAPK, and NF-$\kappa$B signaling pathways in human airway epithelial cells," *Biochemical and Biophysical Research Communications*, vol. 512, no. 1, pp. 53–59, 2019.

[70] J. Wang, Y. Li, P. Zhao et al., "Exposure to air pollution exacerbates inflammation in rats with preexisting COPD," *Mediators of Inflammation*, vol. 2020, Article ID 4260204, 12 pages, 2020.

[71] D. A. Groneberg, P. R. Eynott, T. Oates et al., "Expression of MUC5AC and MUC5B mucins in normal and cystic fibrosis lung," *Respiratory Medicine*, vol. 96, no. 2, pp. 81–86, 2002.

[72] M. O. Henke, A. Renner, R. M. Huber, M. C. Seeds, and B. K. Rubin, "MUC5AC and MUC5B mucins are decreased in cystic fibrosis airway secretions," *American Journal of Respiratory Cell and Molecular Biology*, vol. 31, no. 1, pp. 86–91, 2004.

[73] D. H. Kim, H.-S. Chu, J. Y. Lee, S. J. Hwang, S. H. Lee, and H.-M. Lee, "Up-regulation of MUC5AC and MUC5B mucin genes in chronic rhinosinusitis," *Archives of Otolaryngology-Head and Neck Surgery*, vol. 130, no. 6, pp. 747–752, 2004.

[74] S. T. Ballard and D. Spadafora, "Fluid secretion by submucosal glands of the tracheobronchial airways," *Respiratory Physiology & Neurobiology*, vol. 159, no. 3, pp. 271–277, 2007.

[75] I. Ueki, V. F. German, and J. A. Nadel, "Micropipette measurement of airway submucosal gland secretion. Autonomic effects," *American Review of Respiratory Disease*, vol. 121, no. 2, pp. 351–357, 1980.

[76] M. A. Haxhiu, B. Haxhiu-Poskurica, V. Moracic, W. A. Carlo, and R. J. Martin, "Reflex and chemical responses of tracheal submucosal glands in piglets," *Respiration Physiology*, vol. 82, no. 3, pp. 267–277, 1990.

[77] L. Trout, M. R. Corboz, and S. T. Ballard, "Mechanism of substance P-induced liquid secretion across bronchial epithelium," *American Journal of Physiology-Lung Cellular and Molecular Physiology*, vol. 281, no. 3, pp. 639–645, 2001.

[78] J. E. Phillips, J. A. Hey, and M. R. Corboz, "Tachykinin $NK_3$ and $NK_1$ receptor activation elicits secretion from porcine airway submucosal glands," *British Journal of Pharmacology*, vol. 138, no. 1, pp. 254–260, 2003.

[79] K. Matsumoto, T. Hosoya, K. Tashima, T. Namiki, T. Murayama, and S. Horie, "Distribution of trans ient receptor potential vanilloid 1 channel expressing nerve fibers in mouse rectal and colonic enteric nervous system: relationship to peptidergic and nitrergic neurons," *Neuroscience*, vol. 172, pp. 518–534, 2011.

[80] Z. Ji, Z. Wang, Z. Chen et al., "Melatonin attenuates chronic cough mediated by oxidative stress via transient receptor potential melastatin-2 in Guinea pigs exposed to particulate

matter 2.5," *Physiological Research*, vol. 67, no. 2, pp. 293–305, 2018.

[81] R. Fan, Q. Ren, T. Zhou et al., "Determination of endogenous substance change in $PM_{2.5}$-induced rat plasma and lung samples by UPLC-MS/MS method to identify potential markers for lung impairment," *Environmental Science and Pollution Research*, vol. 26, no. 21, p. 22040, 2019.

[82] C. S. Weldy, I. P. Luttrell, C. C. White et al., "Glutathione (GSH) and the GSH synthesis gene Gclm modulate plasma redox and vascular responses to acute diesel exhaust inhalation in mice," *Inhalation Toxicology*, vol. 25, no. 8, pp. 444–454, 2013.

[83] D. J. Tumes, J. Cormie, M. G. Calvert et al., "Strain-dependent resistance to allergen-induced lung pathophysiology in mice correlates with rate of apoptosis of lung-derived eosinophils," *Journal of Leukocyte Biology*, vol. 81, no. 6, pp. 1362–1373, 2007.

[84] S. Okada, H. Kita, T. J. George, G. J. Gleich, and K. M. Leiferman, "Migration of eosinophils through basement membrane components in vitro: role of matrix metalloproteinase-9," *American Journal of Respiratory Cell and Molecular Biology*, vol. 17, no. 4, pp. 519–528, 1997.

[85] F. Lebargy, E. Lenormand, R. Pariente, and M. Fournier, "Morphological changes in rat tracheal mucosa immediately after antigen challenge," *Bulletin Europeen de Physiopathologie Respiratoire*, vol. 23, no. 5, pp. 417–421, 1987.

[86] H. Y. Choi, T. Y. Jung, S. K. Ku, H. B. Yang, and H. S. Lee, "Toxico-pathological study of p,p-DDE after experimental aerosol exposed to ICR Mouse," *Toxicological Research*, vol. 21, no. 2, pp. 151–160, 2005.

[87] H. Honda, M. Fujimoto, S. Miyamoto et al., "Sputum Leucine-rich alpha-2 glycoprotein as a marker of airway inflammation in asthma," *PLoS One*, vol. 11, no. 9, Article ID e0162672, 2016.

[88] Y. C. Chen, S. Y. Lin-Shiau, and J. K. Lin, "Involvement of reactive oxygen species and caspase 3 activation in arsenite-induced apoptosis," *Journal of Cellular Physiology*, vol. 177, no. 2, pp. 324–333, 1998.

[89] Y.-C. Chen, S.-C. Shen, W.-R. Lee et al., "Emodin induces apoptosis in human promyeloleukemic HL-60 cells accompanied by activation of caspase 3 cascade but independent of reactive oxygen species production," *Biochemical Pharmacology*, vol. 64, no. 12, pp. 1713–1724, 2002.

[90] G. Nunez, M. A. Benedict, Y. Hu, and N. Inohara, "Caspases: the proteases of the apoptotic pathway," *Oncogene*, vol. 17, no. 25, pp. 3237–3245, 1998.

[91] K. L. Barrett, J. M. Willingham, A. J. Garvin, and M. C. Willingham, "Advances in cytochemical methods for detection of apoptosis," *Journal of Histochemistry and Cytochemistry*, vol. 49, no. 7, pp. 821–832, 2001.

[92] X. Li, Z. Ding, C. Zhang et al., "MicroRNA-1228(*) inhibit apoptosis in A549 cells exposed to fine particulate matter," *Environmental Science and Pollution Research*, vol. 23, no. 10, Article ID 10103, 2016.

[93] K. Watanabe, T. Kawamori, S. Nakatsugi, and K. Wakabayashi, "COX-2 and iNOS, good targets for chemoprevention of colon cancer," *BioFactors*, vol. 12, no. 1-4, pp. 129–133, 2000.

[94] S. Chell, A. Kadi, A. Caroline Williams, and C. Paraskeva, "Mediators of PGE2 synthesis and signalling downstream of COX-2 represent potential targets for the prevention/treatment of colorectal cancer," *Biochimica et Biophysica Acta (BBA)-Reviews on Cancer*, vol. 1766, no. 1, pp. 104–119, 2006.

[95] M. He, T. Ichinose, S. Yoshida et al., "PM2.5-induced lung inflammation in mice: differences of inflammatory response in macrophages and type II alveolar cells," *Journal of Applied Toxicology*, vol. 37, no. 10, pp. 1203–1218, 2017.

[96] C. Zou, H. Yang, L. Cui, X. Cao, H. Huang, and T. Chen, "Potential hazardous effects of printing room $PM_{2.5}$ exposure include promotion of lung inflammation and subsequent injury," *Molecular Medicine Reports*, vol. 22, no. 4, pp. 3213–3224, 2020.

[97] M. M. Mohy El-Din, A. M. Senbel, A. A. Bistawroos et al., "A novel COX-2 inhibitor pyrazole derivative proven effective as an anti-inflammatory and analgesic drug," *Basic and Clinical Pharmacology and Toxicology*, vol. 108, no. 4, pp. 263–273, 2011.

[98] T. P. Hamsa and G. Kuttan, "Evaluation of the anti-inflammatory and anti-tumor effect of *Ipomoea obscura* (L) and its mode of action through the inhibition of proinflammatory cytokines, nitric oxide and COX-2," *Inflammation*, vol. 34, no. 3, pp. 171–183, 2011.